Received May 15, 2021, accepted June 25, 2021, date of publication July 1, 2021, date of current version July 12, 2021.

Digital Object Identifier 10.1109/ACCESS.2021.3093954

Power Losses Reduction of Solar PV Systems Under Partial Shading Conditions Using Re-Allocation of PV Module-Fixed Electrical Connections

RUPENDRA KUMAR PACHAURI[1], ISHA KANSAL[1], THANIKANTI SUDHAKAR BABU[2,3], (Senior Member, IEEE), AND HASSAN HAES ALHELOU[4,5], (Senior Member, IEEE)

[1]Department of Electrical and Electronics Engineering, School of Engineering, University of Petroleum and Energy Studies, Dehradun 248007, India
[2]Department of Electrical and Electronics Engineering, Chaitanya Bharathi Institute of Technology, Hyderabad 500075, India
[3]Department of Electrical and Electronics Engineering, Nisantasi University, 34398 Istanbul, Turkey
[4]Department of Electrical Power Engineering, Faculty of Mechanical and Electrical Engineering, Tishreen University, Lattakia 2230, Syria
[5]School of Electrical and Electronic Engineering, University College Dublin, Dublin, D04 V1W8 Ireland

Corresponding authors: Hassan Haes Alhelou (alhelou@ieee.org) and Thanikanti Sudhakar Babu (sudhakarbabu66@gmail.com)

ABSTRACT The paper gives a review of the investigation, which is being imported under different shading scenarios on the solar photovoltaic (PV) array arrangements. Under non-uniform irradiations, the authors pursue voluminous interpretation to scrutinize the mismatch power losses (PL) in PV array systems. In addition to power, the partial shading also reveals non-linearity along with multiple maximum power points (MPP) on performance curves *i.e.* power-voltage (P-V) and current-voltage (I-V). The inspection of the optimal layout of PV modules during the study helps us to extract maximum power and reduce the number of power peaks, when arranged in an array under partial shading conditions (PSCs). In the vicinity of PV array configurations such as series-parallel (SP), honey-comb (HC), bridge-link (BL), total cross-tied (TCT), and hybrid series-parallel-Total cross-tied (SP-TCT), bridge link-honey comb (BL-HC), and bridge link-total cross-tied (BL-TCT) are considered to investigate the performance under shadowing conditions. Moreover, Latin square (LS) puzzle is introduced to reconfigure the PV array and extensive comprehensive comparison with conventional is presented and entitled as ''LS-TCT'' configuration. The MATLAB/Simulink environment helps in modelling all the considered PV array configurations. The recommended LS-TCT configuration is turned out to be superior (for MATLAB/Simulink study) among all configurations during PSCs in terms of location of global maximum power point (GMPP), minimized PL and improved fill factor (FF). To show the superiority of proposed Shape-do-Ku (SPDK) puzzle based configuration, an experimental comparison is shown with conventional TCT and LS-TCT, Su-do-Ku (SDK) puzzle based configurations under new shading pattern-4. In addition, presented experimental study is validated the results obtained during MATLAB/Simulink study.

INDEX TERMS Solar energy, photovoltaic system, shading effect, maximum power, and shade dispersion.

I. INTRODUCTION

In this era, when the repository of fossil fuels is a deficit and limitedly constrained, the rejuvenated analyst needs to explore productive renewable energy (RE) sources. In the framework of the optimum availability of bio-fuel cell energy, wind turbines, and PV systems are emerging RE sources of energy without denying the fact that they have their own limitations towards environmental aspects [1].

PV technology confronts enormous issues due to numerous known and un-acquainted causes' e.g. mal-function and climatic contaminants. In the modern consequence,

The associate editor coordinating the review of this manuscript and approving it for publication was Salvatore Favuzza.

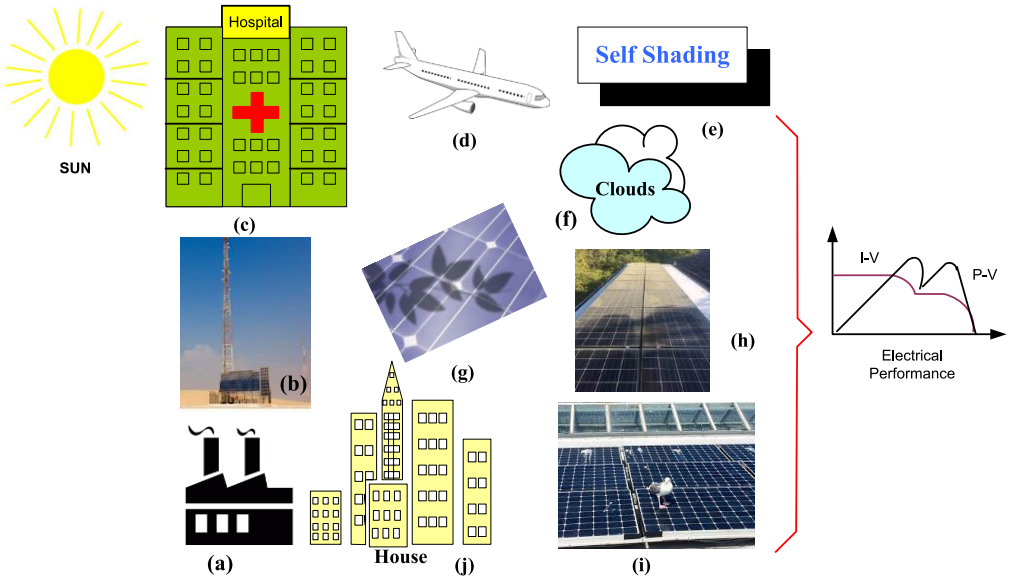

FIGURE 1. Major causes of PSCs and impact on I-V and P-V curves.

the restrictions associated with environmental are rapidly growing due to dust, which is accumulated on the panel surface. The reasons behind the formation of diverse shadows on the surface of PV plants may be due to clouds shifting, neighboring trees, and upraised buildings especially in metropolitan areas [2]. Recently, behavioral enhancement in PV technology has been a quite fascinating area of research with the amendment in electrical connections of PV modules to enhance PV system performance [3]. The PV modules of an array are organized in series, parallel, SP, BL, TCT, and HC configurations [4], but the rearrangement techniques of PV modules are adopted for the performance enrichment in contrast with the conventional ones. The root cause and impact of PSCs on PV system performance are shown in Fig. 1 as,

Presently, researchers are exploring ideas to mend the performance of PV systems under PSCs by using mathematical puzzle-based arrangement of PV modules ($m \times n$) in an array. Various applicable methods are available in the current circumstances to reconfigure PV array systems by altering physical position of module with fixed electrical connections.

The module arrangement in a PV array exists in series and/or parallel to fulfill the load power requirement. In times, when one or more solar panels are shaded, substantially PV performance decreases. In [5], the authors have done comprehensive investigation based on performance outcomes *e.g.* PL, FF, and GMPP locations under the four kinds of shading instances such as long narrow (LN), long wide (LW), short narrow (SN) and short wide (SW). Rearranging the traditional TCT arrangements based on Su-Do-Ku game puzzle for extensive analysis. The maximum power produced by Su-Do-Ku configured structure is 4532W with a power enhancement of 26.1% over TCT configuration. In experimental approach, local and GMPPs are recognized and validated through estimated power as 150W under shading circumstances with the MATLAB/Simulink study [6]. Three series-connected PV panels are believed to determine the effect of irradiation under a non-uniform state at the GMPP site and power output is observed as 165W [7]. In order to achieve the MPPT during the shaded SP, TCT, and BL arranged PV modules (2×4), an experimental and MATLAB/Simulink studies are conducted for validation outcome. It is determined that the TCT arrangement has the best results compared to other modules with a power output of 678.40W [8] and when arranged in 4×4 array produces a power of 2.86KW [9]. The authors of [10], [11] have developed 3×3 SP configured PV array to demonstrate the shadow's effect on the P-V curve. Moreover, GMPP location is observed as 40W.

In [12], three shading circumstances *i.e.* 100%, 66.66%, and 33.3% insolation levels, the author inspected the series and parallel arrangements with grid integration. The outcomes for enhanced FF of 64.54%, low mismatch losses (MML), and GMPP location is noted as 290.5W. For testing of 230W PV panels (eight numbers) arranged in series connections and conducted under three shading test cases in both simulation and experimental aspects. The placement of the bypass diode with the PV system is evaluated during the research to reduce the shadow effect [13]. The optimal interconnection technique is used to scatter the shadow impact on the TCT configured PV array and compared with the outcomes with Su-Do-Ku puzzle in terms of enhanced power of 4802W [14]. For comprehensive research under PSCs, PV array settings defined as series, parallel, SP, TCT, BL, HC, and suggested new PV array setup are regarded in [15]. Compared to others, the proposed 'novel' configuration has a stronger performance. An improved Su-Do-Ku model is

obtained from existing Su-Do-Ku PV model in [16] to analyze the efficiency under four shadowing instances such as SW, LW, SN and LN. In addition, Su-Do-Ku based configuration has the highest power as 1250W and lowest PL among all the experiment instances [17].

In [18], the authors have analyzed TCT and Su-Do-Ku puzzle based reconfigured TCT (RTCT) array systems under passing clouds as a shadow impact on the 6 × 6 size PV system with estimated GMPP as 1160W. Under the distinctive shadow motifs, the performance of standard TCT and Su-Do-Ku puzzle-based RTCT setup is compared, and found enhanced GMPP as 2278W [19]. Results from TCT, SP-TCT, and Su-Do-Ku connections are analyzed. In which, Su-Do-Ku configured PV array have stronger findings as improved FF and less numbers of MPPs on P-V curve. Under shading cases *i.e.* SW, LW, SN, and LN, the production strength of a 7 × 5 PV system increased in terms of maximum power to 73.55W by using various settings such as electrical panel setup and physical re-allocation of PV module and fixed electrical connection [20]. Moreover, Futoshiki arrangement of 5 × 5 PV system is investigated and it has been found 64.87W as power output [21]. Optimum PV panel arrangement in an array are chosen and contrasted under the predefined shading impacts with SP and TCT interconnections. The TCT has highest power as 4419W [22]. In this study [23], author proposed a 6 × 4 MATLAB/Simulink model of an array to implement different configurations *i. e.* TCT, and hybrid SP-TCT, BL-TCT, BL-HC and novel structure (NS) at four distinct insolation levels such as 350W/m^2, 500W/m^2, 800W/m^2, and 1000W/m^2. The experimental analysis leads the author to observe that number of GMPPs compared to TCT. In [24], author have done both simulation and experimental analysis of 6 × 6 size PV array arranged in TCT and magic square (MS) arrangements. The authors have observed that the highest GMPP location as 300W at irradiation levels from 500-1000W/m^2 in the case of MS configuration.

In [25], the author has considered distinct and rational accelerating shading methodologies such as left to right, bottom to top and diagonally multi-story building pattern for amending the behavioural evaluation of TCT configuration over the LS puzzle pattern. The performance parameters such as FF, PL, and GMPP are visualized for TCT and LS-TCT configurations and thus found LS-TCT to be superior with 78.7%, 330W, and 2279W respectively. The author of [26] has done a comprehensive comparison under different shadowing scenarios and thus analysed that new modified Su-Do-Ku configuration has highest GMPP as 26.9%, 30.3%, 30.8%, 16.8%, 4.2%, and 6.3% compared to conventional SP, BL, HC, TCT and Su-Do-Ku PV array interconnections. The authors of [27] used ODD-EVEN (OE) techniques for dispersing high shades on entire PV array by reconfiguring the conventional TCT connections. It has been observed that power enhancement (PE)of the proposed OE configuration is achieved higher side compared to SP, BL and TCT as 30.88%, 14.31%, 8.47%, and 2.18% respectively.

In [28], the authors have given a unique approach of Skyscraper puzzle-based 9 × 9 PV configuration and tested under LN, SW, SN and LN shading scenarios. It is found that the GMPP location is higher side as compared to TCT, Dominance square and Su-Do-Ku (22.36%, 43.36%, and 39.31%) arrangement respectively. The authors in [29], investigated Su-Do-Ku based BL-TCT topology and observed that the power produced as 44.31W by the proposed configuration at different irradiations. The authors in [30] has investigated PV system performance under irregular solar irradiance (400-1000W/m^2) on conventional PV configurations i.e. SP, HC, BL, and TCT, reconfigured method (RM). The author [31] have discussed wide shade dispersion and introduced FRA, SMO algorithm, and RAO algorithm using the same which has allowed him to magnify power by 13%, 11%, and 9% respectively when contrasted with 9 × 9 size TCT, CS, and GA topologies. Under non-uniform irradiation levels of 200W/m^2, 400W/m^2, 500W/m^2, 600W/m^2 and 900W/m^2 different performance parameters i. e. FF, ML, %PL, and %PE are observed and thus concluded full reconfigured array with higher power and reduced MPP. The game puzzles are used to reconfigure the conventional TCT PV array configurations. In this paper, the PV array configurations such as LS-TCT is considered. The property of shade dispersion is always vary based on set of integer numbers to design the game puzzle. 9 × 9 size PV array is investigated to show the comparison with existed TCT configuration under four shading scenarios as SW, LW, SN and LN. The minimized PL are observed as 6.75W, 3.98W, 4.68W and 6.95W respectively [32]. Another technique has proposed [33] hybrid reconfiguration algorithm, this technique investigate which step matrix is more efficient. The presented technique decrease the effect of partial shading in the power output and circuit. In [34], the Coyote Optimization Algorithm (COA) is used to reconfigure the PV array and compared to TCT, Su-Do-Ku, flower pollination algorithm (FPA), butterfly optimization algorithm (BOA), and marine predictor algorithm (MPA) PV array configurations. Under four shading scenarios (SW, SN, LW and LN), the COA-based GMPP configuration is found to be 11kW, 1.08kW, 1.45kW and 1.560kW respectively. Another Luo Shu technique [35] has been used for prevent MML, output power and other topology of PV array under shading area. Comprehensive comparison is carried out between TCT, Su-Do-Ku, Dominance square (DS), Competence square (CS) and proposed Luo Shu PV array configurations under shading scenarios. Through, that obtained I-V and P-V curves clearly shown higher performance of Luo Shu PV array.

A. NOVELTY OF WORK

The goal of this paper is to organize the position of modules physically without altering the electrical links to improve PV performance under PSCs. The game puzzles e.g. LS-TCT, SDK, SPDK configurations are tested to shown an efficient result due to subsequent reasons.

(a) The recommended LS-TCT based electrical connections highly capable to disperse the shadow patterns 1-3 on top of the existed PV modules of an array (during MATLAB/Simulink study).
(b) Using the shade dispersion methodology, the LS-TCT based electrical connections produce large power in comparison with the classical (SP, BL, HC, TCT), hybrid (BL-HC, BL-TCT, and SP-TCT) connections.
(c) An immense comparative study is being carried on the considered classical, hybrid, and proposed LS-TCT based electrical connections under the distinguish shading cases to test the adaptability and feasibility in terms of output power at GMPP, FF and minimized PL.
(d) In addition, LS-TCT is compared with SDK and SPDK puzzle based PV array configurations under shading pattern-4.
(e) The experimental validation is carried out to show the efficient performance of SPDK based PV array configuration.

II. PV SYSTEM TECHNOLOGY AND ARRAY TOPOLOGIES

Strategies assumed in the proposed work for modelling of PV system is clarified in the section given below,

A. MODELING OF THE PV SYSTEM

The arrangement of PV modules connected into SP produces high power generation as presented in Fig. 2.

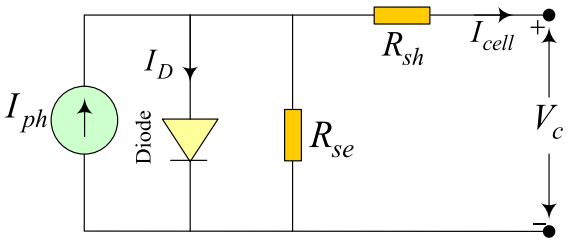

FIGURE 2. Equivalent circuit of PV cell.

Solar PV voltage of a unit cell (V_C) depends upon solar irradiation and is the function of current (I_{SC}) which can be conveyed through Eq. (1) as,

$$V_C = \frac{AkT_C}{e} \ln\left(\frac{I_{ph} + I_D + I_{cell}}{I_D}\right) - \left(\frac{R_{se}R_{sh}}{R_{se} + R_{sh}}\right) I_{cell} \quad (1)$$

The solar irradiation level (S_C) and ambient temperature (T_a) are the two factors varying the operating temperature (T_C) of PV cell. Voltage and current correction factors *i.e.* C_{TV} and C_{TI} respectively shown in Eq. (2) as,

$$C_{TV} = 1 + \beta_T\,(T_a - T_x)\ \&\ C_{TI} = 1 + \frac{\gamma_T}{S_C}\,(T_x - T_a) \quad (2)$$

C_{SV} & C_{SI} are two correction factors which are responsible for the outcome of irradiation level (S_x). The correction factors C_{SV}, for voltage and C_{SI}, for photocurrent can be conveyed through in Eq. (3) as,

$$C_{SV} = 1 + \beta_T\alpha_S\,(S_x - S_c)\ \&\ C_{SI} = 1 + \frac{1}{S_c}\,(S_x - S_c) \quad (3)$$

TABLE 1. Parameters of commercial available pv module [23].

Parameters	Values
V_{OC}	44.2 V
V_m	35.8 V
I_{SC}	5.2 A
I_m	4.75 A
P_m	170 W

where, S_c and S_x referred to the solar and actual irradiation level respectively. The actual values referring to PV cell such as photocurrent *i. e.* I_{phx} and its voltage *i. e.* V_{cx} can be determined through correction factors C_{TV}, C_{TI}, C_{SV} and C_{SI} can be expressed in Eq. (4) as

$$V_{cx} = C_{TV}C_{SV}V_C\ \&\ I_{phx} = C_{TI}C_{SI}I_{ph} \quad (4)$$

Commercially available PV module specifications at standard test scenarios are considered for MATLAB/Simulink modelling to investigate PV array systems under PSCs as,

B. PV ARRAY CONFIGURATIONS

1) CONVENTIONAL PV ARRAY CONFIGURATIONS

Fig. 3(a)-(h) shows distinct variants of PV array configurations *i.e.* SP, BL, HC, TCT, hybrid SP-TCT, BL-HC, BL-TCT, and proposed LS-TCT. Fig. 3(a)-(c) represents conventional SP, BL, and HC configuration for an array of size 4×4 of PV panels where its conduct is measured in relation to GMPP and FF. Fig. 3(d) represents TCT arrangement, for array size 4×4 of PV panels, which is obtained by ties connected across individual rows of interconnections to produce high power. The recombination of classical SP, BL, and HC along with TCT topology, represents the hybrid topology of PV array and is obtained in Fig. 3(e)-(g) below.

2) LS PUZZLE BASED PV ARRAY CONFIGURATION

Fig. 3(h) constitutes the unique proposal of LS-TCT puzzle pattern-based PV array topology, where the positions of PV modules are reallocated according to modified TCT, unchanging the electrical interconnections. In this arrangement, the first digit and second digit of each module in a PV array denote the row and the column respectively.

LS is an ancient puzzle where users try to find out how many integer numbers can be arranged in a specified number of rows and columns. Moreover, each symbol appears only once in each row and column in the matrix and developed by Leonard Euler. Property of such a puzzle with higher shading dispersion during the reconfiguration of PV array under the PSCs [32].

The property of shade dispersion is always vary based on set of integer numbers to design the game puzzle. So, the placement of LS puzzle having different properties with various placement possibilities of integer number (1-4). The methodology to reconfigure PV array based on LS puzzle is shown in Fig. 3(k).

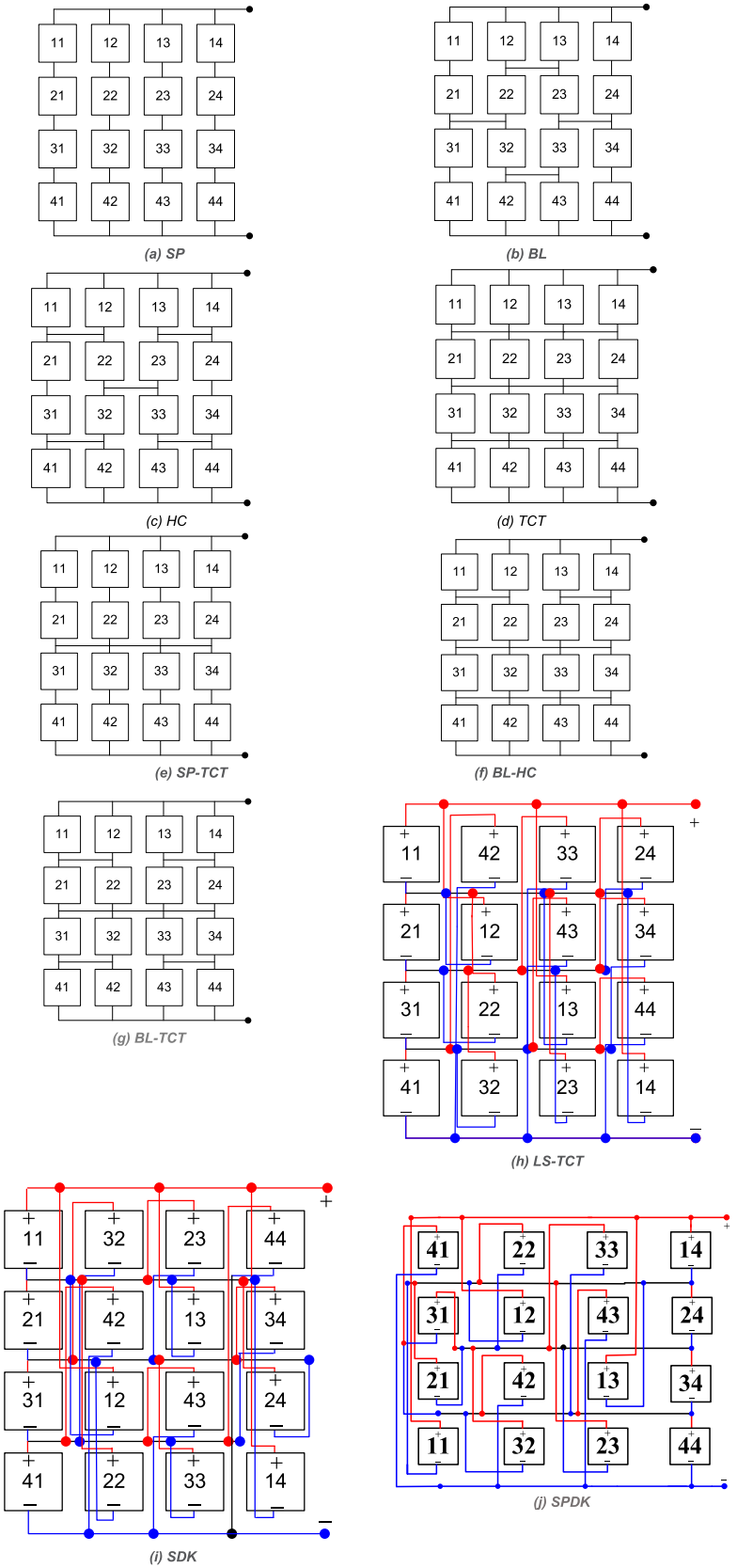

FIGURE 3. (a)-(m). Conventional, hybrid, game puzzle based PV array configurations and flow charts of game puzzles.

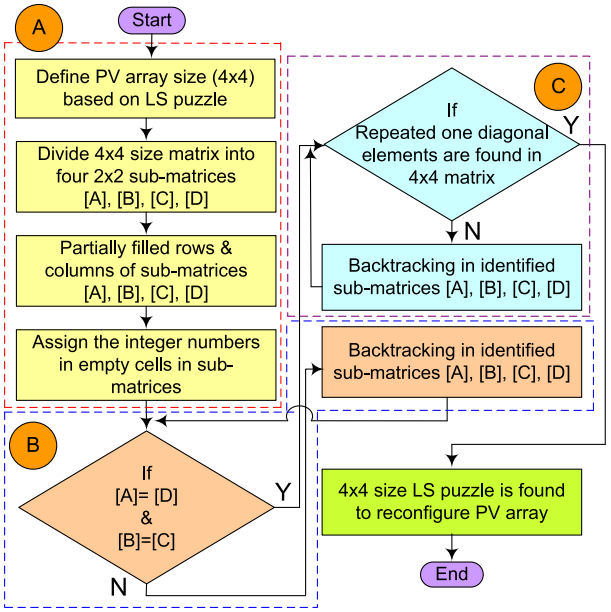

(k) Flow chart for LS methodology to design 4x4 size PV array

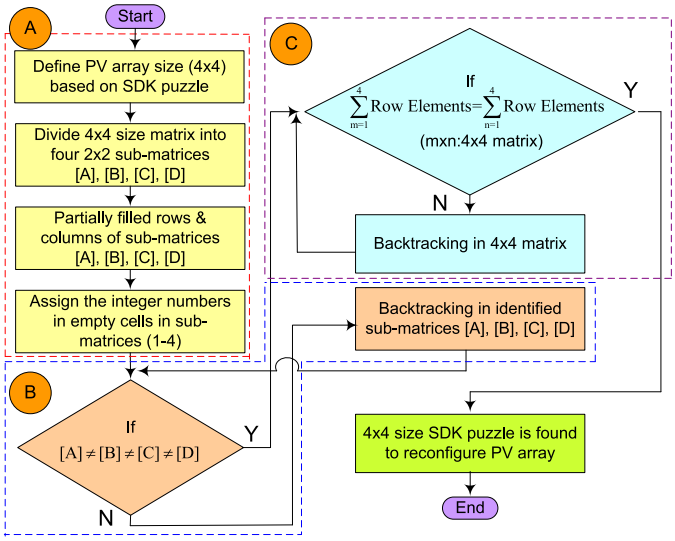

(l) Flow chart for SDK methodology to design 4x4 size PV array

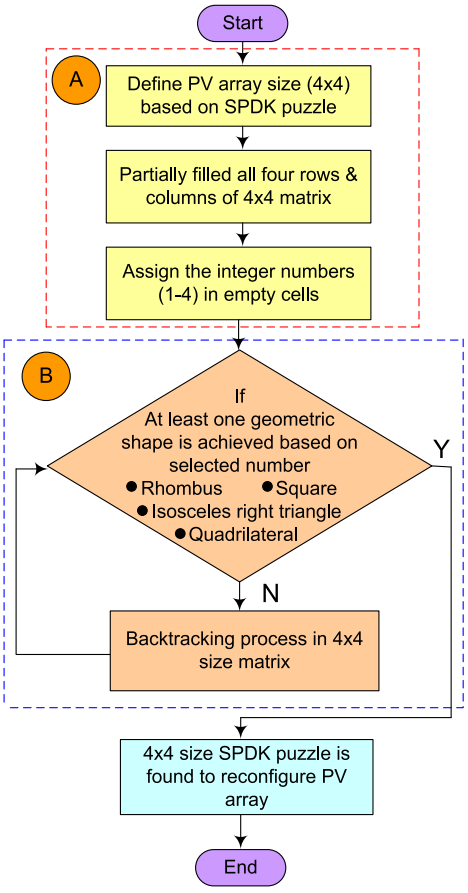

(m) Flow chart for SPDK methodology to design 4x4 size PV array

FIGURE 3. *(Continued.)* **(a)-(m). Conventional, hybrid, game puzzle based PV array configurations and flow charts of game puzzles.**

3) SU-DO-KU PUZZLE BASED PV ARRAY CONFIGURATIONS

For shade dispersion, this SDK puzzle is introduced first to reconfigure PV array in 2013 [5] and tested under PSCs. The 4×4 size PV array is reconfigured using set of rules with integer numbers (1-4) in each row-column of the matrix. The potential electrical connections and design methodology are shown in Fig. 3(i) and Fig. 3(l), respectively.

4) SHAPE-DO-KU PUZZLE BASED PV ARRAY CONFIGURATION

The SPDK puzzle is existed in various sizes ($4\times4, 5\times5, 6\times6$) with symmetrical properties and it has no technical relation to the SDK puzzle. But, it is a version of the LS puzzle with the only restriction that each number appear at least single time in each column and row [36]. The PV array is reconfigured in this paper using a 4×4-size SPDK puzzle. Fig. 3(j) and Fig. 3(m) demonstrate the electrical connections and design methodology, respectively.

III. ANALYSIS OF PERFORMANCE PARAMETERS AND SHADING PATTERNS

To prove any method as a superior technique, it's necessary to evaluate its performance parameters. With this notice, in this article authors have considered different performance parameters to assess the superiority of proposed PV array reconfiguration technique. The detailed analysis of these parameters are as follows:

A. PERFORMANCE PARAMETERS

1) POWER LOSS

Fig. 4 depicts different kinds of losses in an array under diverse shading conditions served to investigate PV array performance. The contrast between GMPP and LMPP is the root cause of misleading power. Interconnections among the PV modules are the only factor affecting PV array performance with reference to PL. MML in the PV array can be expressed in Eq. (5) as,

$$PL = Maximum\ power\ at\ the\ standard\ condition - GMP\ under\ diverse\ PSCs \quad (5)$$

2) FILL FACTOR

It has been observed from Fig. 4 that, FF is affected by PL under PSCs. It is observed in the P-V and I-V plots that the I_{SC} & V_{OC} effect the FF directly as shown in Eq. (6).

$$FF = \frac{P_{GMPP}}{V_{OC} I_{SC}} \quad (6)$$

3) PERFORMACE RATIO

At STC, the PR of PV array can be expressed as the ratio of power at GMPP under PSCs and power at normalized condition by eq. (7) as,

$$\%PR = \frac{GMPP\ at\ PSCs}{MPP\ at\ s\tan dard\ condition} \times 100 \quad (7)$$

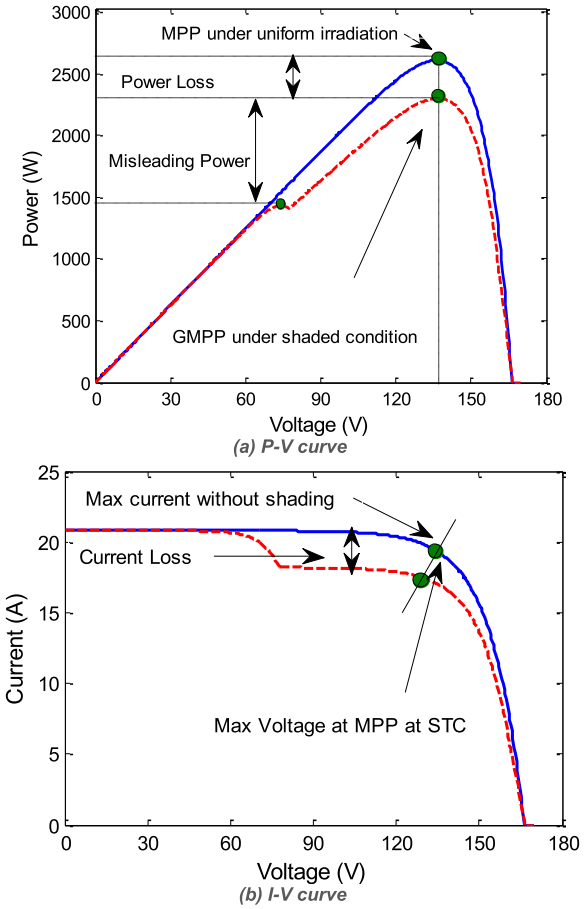

FIGURE 4. (a)-(b). Shading impact on P-V and I-V curves.

B. ANALYSIS OF SHADING SCENARIOS

The paper demonstrates eight forms of arrangements i.e. SP, BL, HC, TCT, BL-HC, BL-TCT, SP-TCT and LS-TCT in each case with three cases in each shading pattern. In the article, three distinct types of shading patterns are distinguished with the help of shadow movements. The irradiation levels such as 1000W/m^2 and 500W/m^2 are considered during the study.

1) SHADING PATTERN-1

It constitutes three cases-1, 2, and 3 with different shadow movements as presented in Fig. 5 as,

Three PV modules of the first, second, and third-row receive uniform solar irradiation of 1000W/m^2. Moreover, in the fourth row, two modules receive irradiation of 500 W/m^2 and the leftover two modules receive 1000W/m^2 of solar irradiation. So, to evaluate the current produced in the first, second, and third row of 4×4 PV array is denoted in Eq. (8)-(13). The current generated under shading case-1 as,

$$\left.\begin{aligned} I_{R_1} = I_{R_2} = I_{R_3} = 4\left(\frac{S_x}{S_{STC}}\right) I_m = \left(\frac{1000}{1000}\right) I_m \\ + \left(\frac{1000}{1000}\right) I_m + \left(\frac{1000}{1000}\right) I_m + \left(\frac{1000}{1000}\right) I_m = 4 I_m \end{aligned}\right\} \quad (8)$$

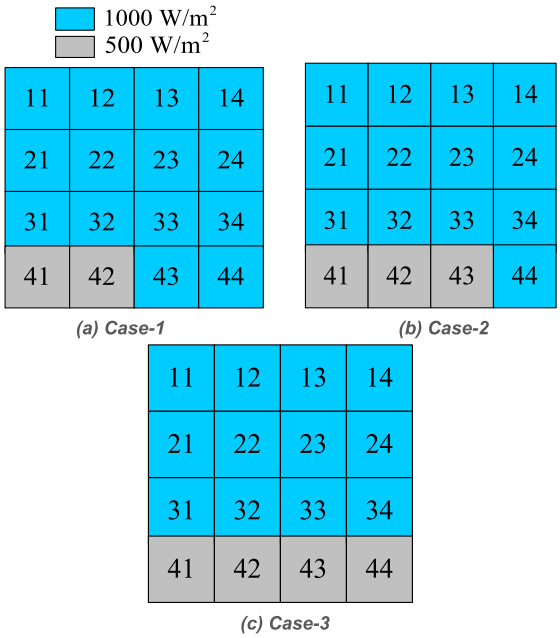

FIGURE 5. (a)-(c). Shading cases 1-3 for pattern-1.

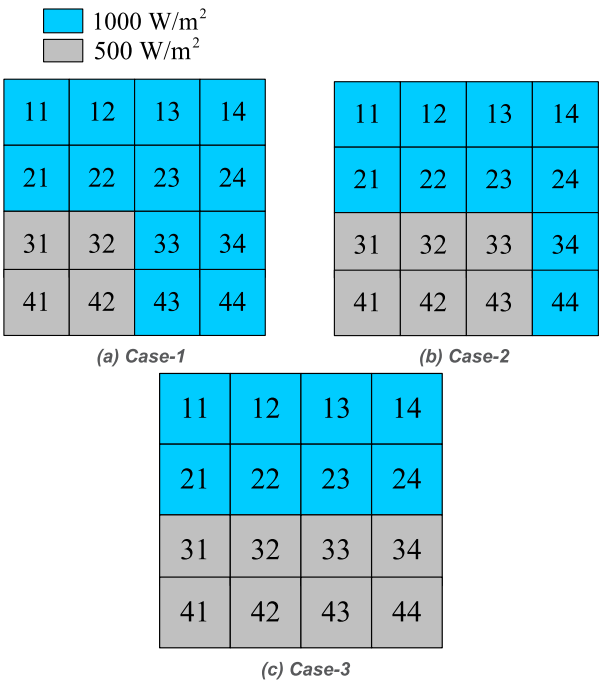

FIGURE 6. (a)-(c). Shading cases 1-3 for pattern-2.

$$I_{R_4} = \left(\frac{500}{1000}\right) I_m + \left(\frac{500}{1000}\right) I_m + \left(\frac{1000}{1000}\right) I_m + \left(\frac{1000}{1000}\right) I_m = 3I_m \Bigg\} \quad (9)$$

Similarly, the current generated under case-2,

$$I_{R_1} = I_{R_2} = I_{R_3} = \left(\frac{1000}{1000}\right) I_m + \left(\frac{1000}{1000}\right) I_m + \left(\frac{1000}{1000}\right) I_m + \left(\frac{1000}{1000}\right) I_m = 4I_m \Bigg\} \quad (10)$$

$$I_{R_4} = \left(\frac{1000}{1000}\right) I_m + \left(\frac{500}{1000}\right) I_m + \left(\frac{500}{1000}\right) I_m + \left(\frac{500}{1000}\right) I_m = 2.5I_m \Bigg\} \quad (11)$$

The generated current in fourth row is calculated as,
Moreover, the current generated under shading case- 3 as,

$$I_{R_1} = I_{R_2} = I_{R_3} = \left(\frac{1000}{1000}\right) I_m + \left(\frac{1000}{1000}\right) I_m + \left(\frac{1000}{1000}\right) I_m + \left(\frac{1000}{1000}\right) I_m = 4I_m \Bigg\} \quad (12)$$

$$I_{R_4} = \left(\frac{500}{1000}\right) I_m + \left(\frac{500}{1000}\right) I_m + \left(\frac{500}{1000}\right) I_m + \left(\frac{500}{1000}\right) I_m = 2I_m \Bigg\} \quad (13)$$

2) SHADING PATTERN-2

The shadow is presumed to be approaching towards right from the leftmost bottom two modules progressing upwards as depicted by cases 1- 3 of Fig. 6 as,

Theoretical analysis of generated current under shading cases 1-3 can be carried out and expressed in Eq. (14)- (19) as,

Generated current for case-1

$$I_{R_1} = I_{R_2} = \left(\frac{1000}{1000}\right) I_m + \left(\frac{1000}{1000}\right) I_m + \left(\frac{1000}{1000}\right) I_m + \left(\frac{1000}{1000}\right) I_m = 4I_m \Bigg\} \quad (14)$$

$$I_{R_3} = I_{R_4} = \left(\frac{500}{1000}\right) I_m + \left(\frac{500}{1000}\right) I_m + \left(\frac{1000}{1000}\right) I_m + \left(\frac{1000}{1000}\right) I_m = 3I_m \Bigg\} \quad (15)$$

Generated current for case-2

$$I_{R_1} = I_{R_2} = \left(\frac{1000}{1000}\right) I_m + \left(\frac{1000}{1000}\right) I_m + \left(\frac{1000}{1000}\right) I_m + \left(\frac{1000}{1000}\right) I_m = 4I_m \Bigg\} \quad (16)$$

$$I_{R_3} = I_{R_4} = \left(\frac{500}{1000}\right) I_m + \left(\frac{500}{1000}\right) I_m + \left(\frac{500}{1000}\right) I_m + \left(\frac{1000}{1000}\right) I_m = 2.5I_m \Bigg\} \quad (17)$$

Generated current for case-3

$$I_{R_1} = I_{R_2} = \left(\frac{1000}{1000}\right) I_m + \left(\frac{1000}{1000}\right) I_m + \left(\frac{1000}{1000}\right) I_m + \left(\frac{1000}{1000}\right) I_m = 4I_m \Bigg\} \quad (18)$$

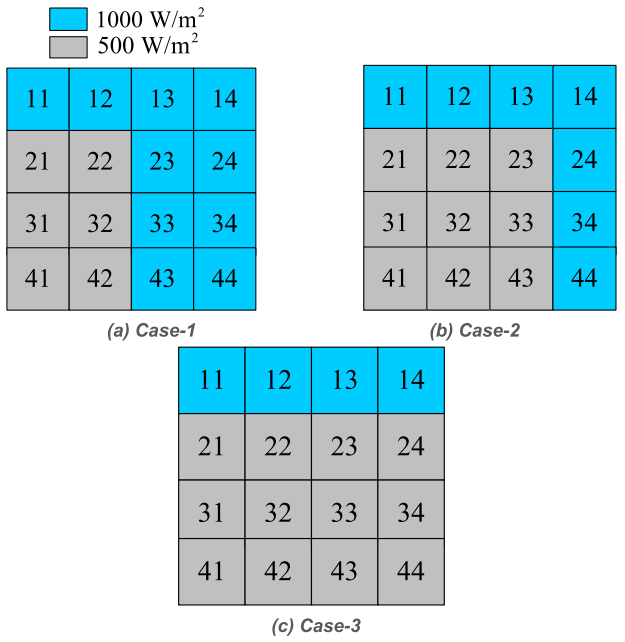

FIGURE 7. (a)-(c). Shading cases 1-3 for pattern-3.

$$\left.\begin{aligned} I_{R_3} = I_{R_4} = \left(\frac{500}{1000}\right) I_m + \left(\frac{500}{1000}\right) I_m \\ + \left(\frac{500}{1000}\right) I_m + \left(\frac{500}{1000}\right) I_m = 2I_m \end{aligned}\right\} \quad (19)$$

3) SHADING PATTERN-3

Considering shading pattern-3, it is observed that there is an upward movement of shadow as we are switching from pattern 1 to 3 of PV array and in each arrangement. The left to right shading on PV modules is shown by cases 1-3 of Fig. 7 as,

Theoretical analysis of generated current under shading cases 1-3 can be expressed in Eq. (20)-(25) as,

Generated current for case-1

$$\left.\begin{aligned} I_{R_1} = \left(\frac{1000}{1000}\right) I_m + \left(\frac{1000}{1000}\right) I_m + \left(\frac{1000}{1000}\right) I_m \\ + \left(\frac{1000}{1000}\right) I_m = 4I_m \end{aligned}\right\} \quad (20)$$

$$\left.\begin{aligned} I_{R_2} = I_{R_3} = I_{R_4} = \left(\frac{500}{1000}\right) I_m + \left(\frac{500}{1000}\right) I_m \\ + \left(\frac{1000}{1000}\right) I_m + \left(\frac{1000}{1000}\right) I_m = 3I_m \end{aligned}\right\} \quad (21)$$

Generated current for case-2

$$\left.\begin{aligned} I_{R_1} = \left(\frac{1000}{1000}\right) I_m + \left(\frac{1000}{1000}\right) I_m + \left(\frac{1000}{1000}\right) I_m \\ + \left(\frac{1000}{1000}\right) I_m = 4I_m \end{aligned}\right\} \quad (22)$$

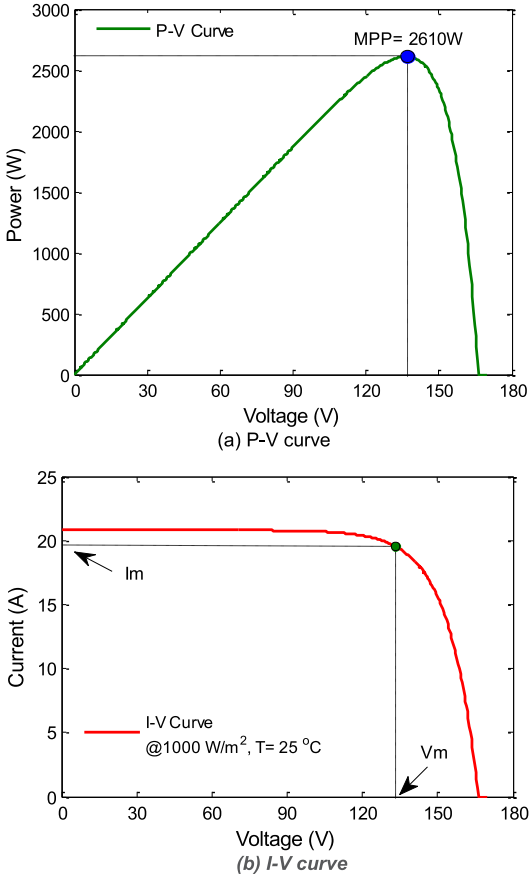

FIGURE 8. (a)-(b). P-V and I-V curves (STC).

$$\left.\begin{aligned} I_{R_2} = I_{R_3} = I_{R_4} = \left(\frac{500}{1000}\right) I_m + \left(\frac{500}{1000}\right) I_m \\ + \left(\frac{500}{1000}\right) I_m + \left(\frac{1000}{1000}\right) I_m = 2.5I_m \end{aligned}\right\} \quad (23)$$

Generated current for case-3

$$\left.\begin{aligned} I_{R_1} = \left(\frac{1000}{1000}\right) I_m + \left(\frac{1000}{1000}\right) I_m + \left(\frac{1000}{1000}\right) I_m \\ + \left(\frac{1000}{1000}\right) I_m = 4I_m \end{aligned}\right\} \quad (24)$$

$$\left.\begin{aligned} I_{R_2} = I_{R_3} = I_{R_4} = \left(\frac{500}{1000}\right) I_m + \left(\frac{500}{1000}\right) I_m \\ + \left(\frac{500}{1000}\right) I_m + \left(\frac{500}{1000}\right) I_m = 2.5I_m \end{aligned}\right\} \quad (25)$$

IV. RESULTS AND DISCUSSION

With the due effect of various PSCs, the following investigations have been demonstrated on various PV array configurations to estimate the extensive performance.

A. P-V AND I-V CURVES AT STC

The single PV module's P-V and I-V curves at STC and insolation levels with power at GMPP as 2610W through MATLAB simulations are presented in Fig. 8 as,

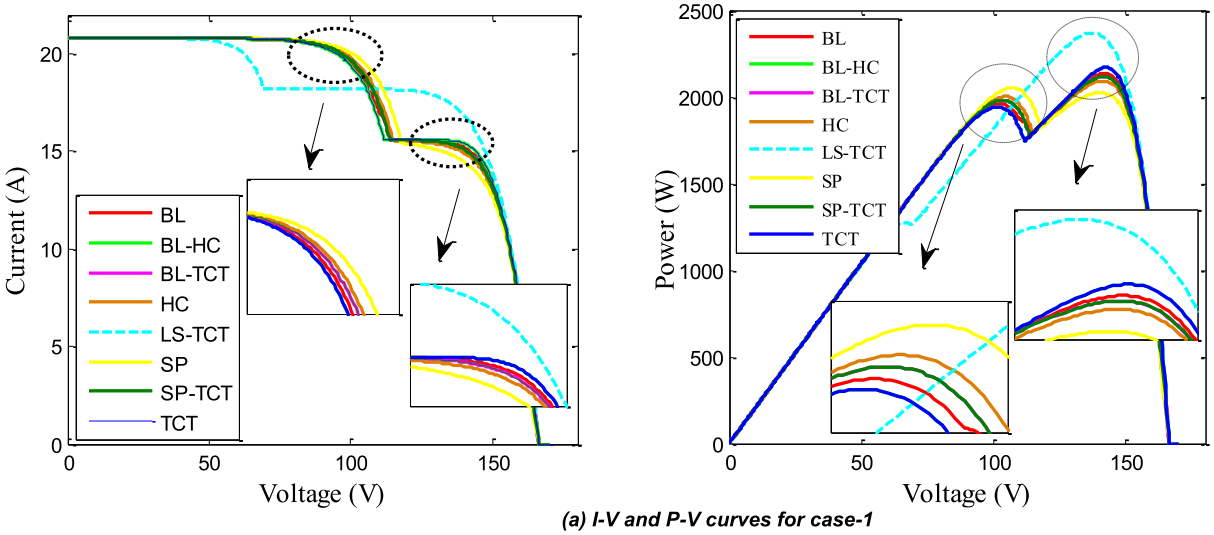

(a) I-V and P-V curves for case-1

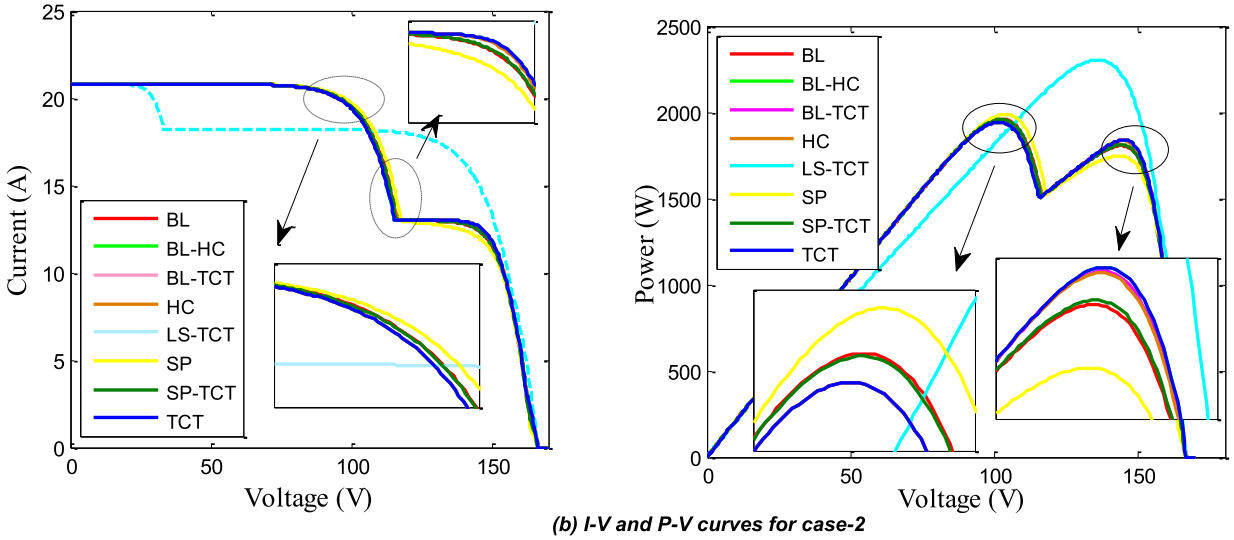

(b) I-V and P-V curves for case-2

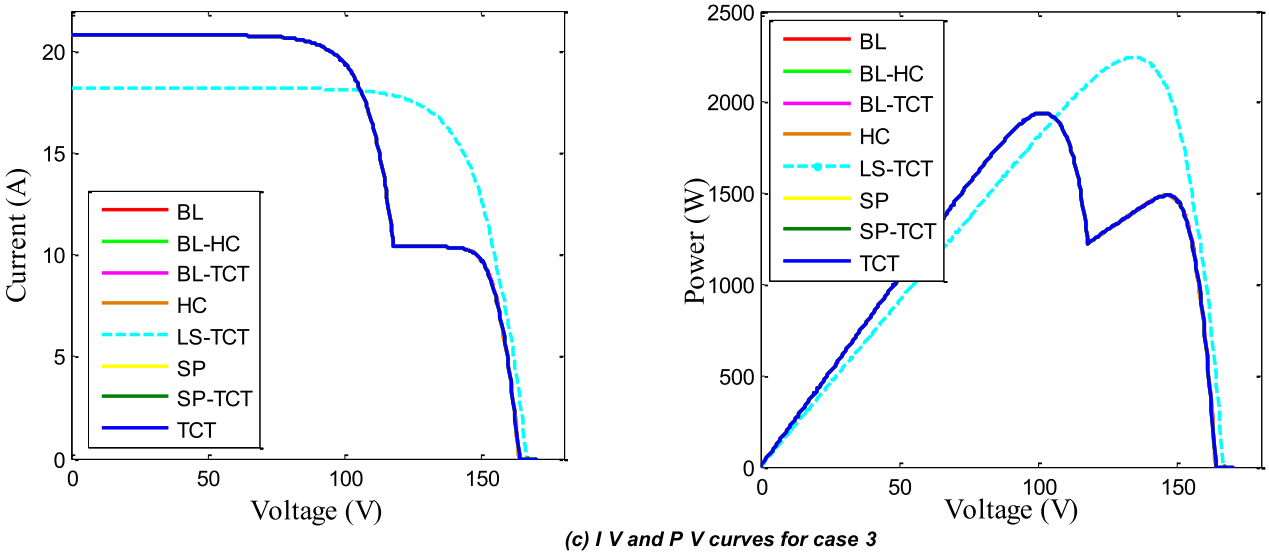

(c) I V and P V curves for case 3

FIGURE 9. (a)-(c). I-V and P-V curves under shading pattern-1.

B. EFFECT ON PV ARRAY CONFIGURATIONS UNDER SHADING PATTERN-1

1) P-V AND I-V CURVES

The I-V and P–V curves of all the possible topologies of PV array undergoing three distinct types of shading patterns from bottom to top including three cases in each pattern (left to right) from cases 1–3 is demonstrated and differentiated through Fig. 9. From Fig. 9(a), it is clearly inferred that two MPPs *i. e.* GMPP and LMPP are existing on the P–V curve for all the topologies. Both MPP's are found to be far apart from each other and lead to a small increase in the consequences of partial shading however the global point for LS-TCT is smooth for case '5a'. The power obtained at GMPP is noticed as 2053W, 2134W, 2091W, 2169W, 2169W, 2118W, 2118W, and 2368W for the SP, BL, HC, TCT, BL-HC, BL–TCT, SP–TCT, and LS-TCT topologies as presented in Fig.10. The P–V curve for the case referred to in Fig. 5(b)-(c) are presented in Fig. 9(b)-(c) respectively. With reference to the shading instance of Fig. 5(c), it has been inspected through Fig. 9(c) that in classical and hybrid topology, the local and global MPP are far apart from each other. The obtained power at GMPP for these two cases are identified as 1988W, 1960W, 1942W, 1942W, 1942W, 1942W, 1958W, 2333W for case '5b' and 1942W, 1942W, 1942W, 1942W, 1942W, 1942W, 1942W, 2247W for case '5c' respectively as shown in Fig. 10.

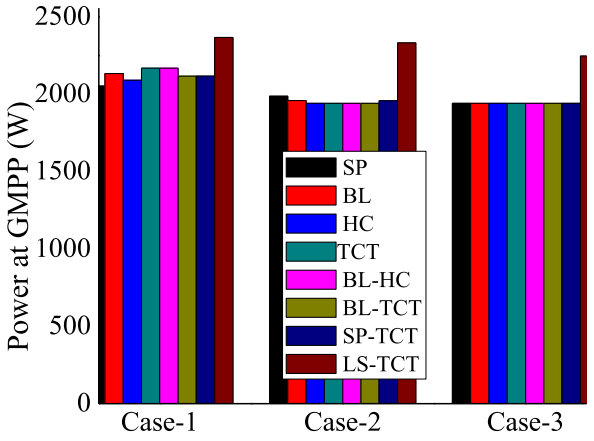

FIGURE 10. Power at GMPP for cases 1-3 under shading pattern-1.

The current, voltage, and power of LS-TCT interconnections are shown in Table 2. The produced power is incremented in few cases of distinct shading scenarios for LS-TCT configurations. Due to the rearrangement of modules, the shadowing consequence of shading pattern-1 gets dispersed over the PV array with an increment in power.

2) POWER LOSS

In each case, the LS-TCT puzzle pattern displays better performance in comparison to SP, BL, HC, TCT, BL-HC, BL–TCT, and SP–TCT when subjected to shade pattern-1. The power losses are expressed using a bar graph and through tabular data presented in Fig. 11 and Table 2 respectively. The PL are observed to be very less in the LS-TCT puzzle configuration under all the shading conditions for pattern-1.

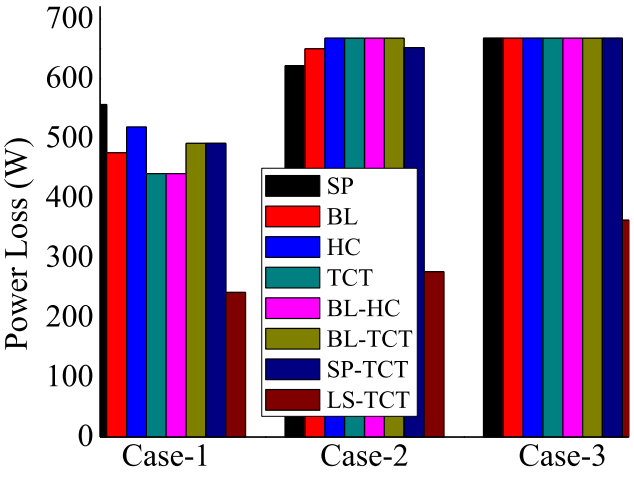

FIGURE 11. Power losses for cases 1-3 under shading pattern-1.

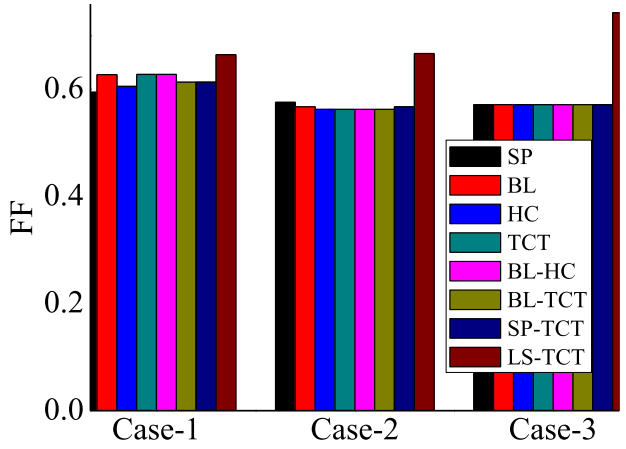

FIGURE 12. FF for cases 1-3 under shading pattern-1.

3) FILL FACTOR

The effect of shade gets escalated with its movement from one end to another on the PV Array resulting in a decrease in FF. Through shading pattern-1 in Fig. 5(a)-(c), it is constituted as a bar graph and presented through Fig. 12. Values corresponding to FF are represented in Table 2 for all the configurations considered in shading pattern-1. It is clearly inferred that FF for LS-TCT topology is superior for the shading pattern-1.

C. EFFECT ON PV ARRAY CONFIGURATIONS UNDER SHADING PATTERN-2

1) P-V AND I-V CURVES

In cases '1-3' of shading pattern- 2, the P–V trait are visible in Fig. 13 of the PV array. On the P–V graph, various MPP's are observed concerning the case represented through

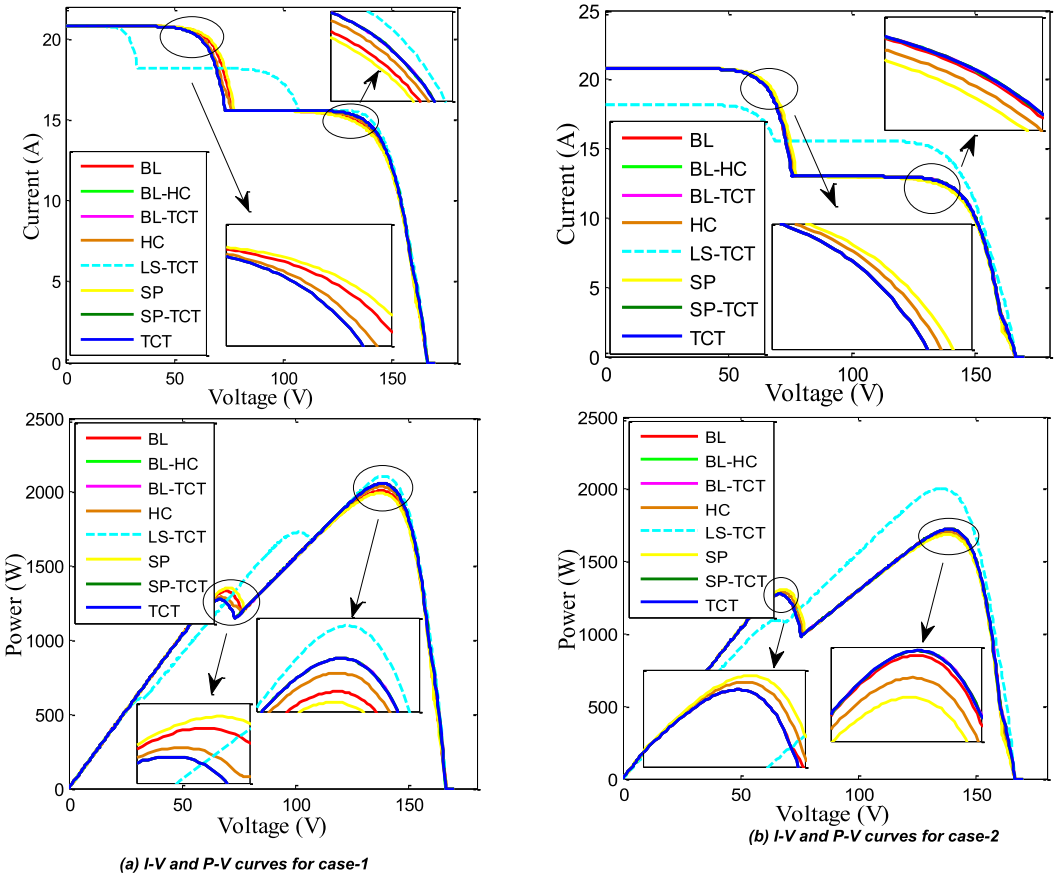

(a) I-V and P-V curves for case-1

(b) I-V and P-V curves for case-2

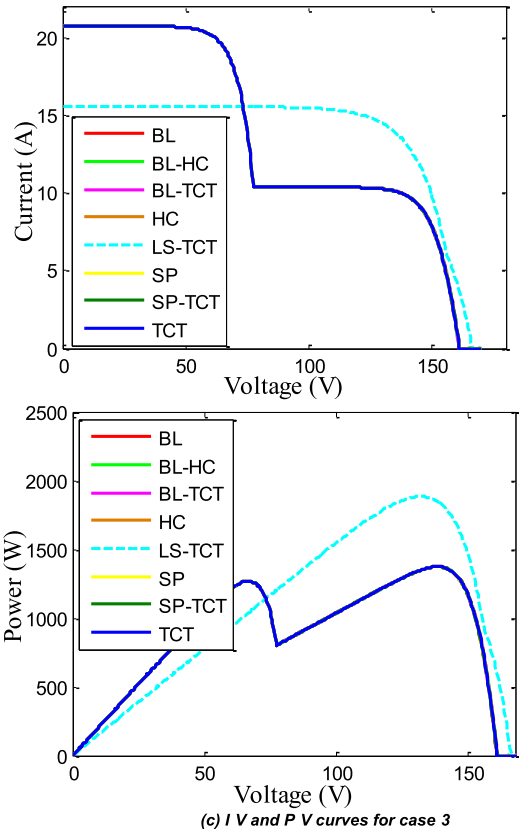

(c) I V and P V curves for case 3

FIGURE 13. (a)-(c). I-V and P-V curves under shading pattern-2.

TABLE 2. Current, voltage, power, PL, mismatch power loss and FF for each configuration under shading pattern-1.

Performance Parameters	Case-1							
	SP	BL	HC	TCT	BL-HC	BL-TCT	SP-TCT	LS-TCT
$V_{OC}(V)$	166.1	166.1	166.1	166.1	166.1	166.1	166.1	166.1
$I_{SC}(A)$	20.8	20.8	20.8	20.8	20.8	20.8	20.8	20.8
$V_m(V)$	107.3	142.3	141	142.4	142.4	141.9	141.9	127.8
$I_m(A)$	19.14	15.23	14.83	15.23	15.23	14.93	14.93	17.96
$P_{GMPP}(W)$	2053	2134	2091	2169	2169	2118	2118	2368
$P_{LMPP}(W)$	2024	1960	2001	1942	1942	1981	1981	1274
$PL(W)$	557	476	519	441	441	492	492	242
FF	0.5944	0.6273	0.6052	0.6277	0.6277	0.6132	0.6132	0.6644
Performance Parameters	**Case-2**							
	SP	**BL**	**HC**	**TCT**	**BL-HC**	**BL-TCT**	**SP-TCT**	**LS-TCT**
$V_{OC}(V)$	166.1	166.1	166.1	166.1	166.1	166.1	166.1	166.1
$I_{SC}(A)$	20.8	20.8	20.8	20.8	20.8	20.8	20.8	20.8
$V_m(V)$	104.5	102.4	101.5	101.5	101.5	101.5	103	136.1
$I_m(A)$	19.03	19.14	19.14	19.14	19.14	19.14	19.02	16.92
$P_{GMPP}(W)$	1988	1960	1942	1942	1942	1942	1958	2333
$P_{LMPP}(W)$	1747	1806	1835	1841	1841	1838	1810	606.7
$PL(W)$	622	650	668	668	668	668	652	277
FF	0.5756	0.5673	0.5623	0.5623	0.5623	0.5623	0.567	0.666
Performance Parameters	**Case-3**							
	SP	**BL**	**HC**	**TCT**	**BL-HC**	**BL-TCT**	**SP-TCT**	**LS-TCT**
$V_{OC}(V)$	163.6	163.6	163.6	163.6	163.6	163.6	163.6	166.2
$I_{SC}(A)$	20.8	20.8	20.8	20.8	20.8	20.8	20.8	18.2
$V_m(V)$	101.5	101.5	101.5	101.5	101.5	101.5	101.5	134.8
$I_m(A)$	19.14	19.14	19.14	19.14	19.14	19.14	19.14	16.67
$P_{GMPP}(W)$	1942	1942	1942	1942	1942	1942	1942	2247
$P_{LMPP}(W)$	1489	1489	1489	1489	1489	1489	1489	0
$PL(W)$	668	668	668	668	668	668	668	363
FF	0.5709	0.5709	0.5709	0.5709	0.5709	0.5709	0.5709	0.7429

Fig. 6(a) - (c). It has been inferred from the graph that local and global MPP are far apart from each other. It is observed with reference to the shading case in Fig. 6(a) that the effect of shading gets escalated as we move on from cases '1-3' on the P-V curve. The obtained power at GMPP is noticed as 1994W, 2010W, 2037W, 2059W, 2059W, 2059W, 2059W and 2108W for SP, BL, HC, TCT, BL-HC, BL–TCT, SP–TCT, and LS-TCT interconnection respectively. For the shading cases presented by Fig. 6(b) and Fig. 6(c), the P–V plot is displayed in Fig. 13(b). The power obtained at GMPP for instance '2' and '3' is observed as 1686 W, 1721W, 1703W, 1725W, 1725W, 1725W, 1725W, 2004W and 1379W, 1379W, 1379W, 1379W, 1379W, 1379W, 1892W for SP, BL, HC, TCT, BL-HC, BL–TCT, SP–TCT and LS-TCT framework respectively as shown in Fig. 14 in the form of bar graph. The power and voltages at GMPP are the parameters for comparison of distinct forms of PV array framework and results are presented through Table 3. The procured result shows that the LS-TCT puzzle pattern generates leading power in comparison to eight 4 × 4 other topologies.

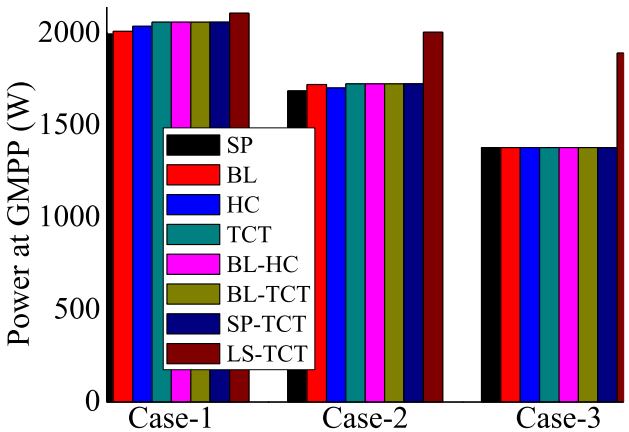

FIGURE 14. Power at GMPP for cases 1-3 under shading pattern-2.

The current, voltage, and power of LS-TCT topology are shown in Table 3. The array's production is incremented in few cases of distinct shading scenarios after the reordering of modules in accordance with LS puzzle pattern.

TABLE 3. Current, voltage, power, PL, mismatch power loss and FF for each topology under shading pattern-2.

Performance Parameters	Case-1							
	SP	BL	HC	TCT	BL-HC	BL-TCT	SP-TCT	LS-TCT
$V_{OC}(V)$	166.2	166.2	166.2	166.2	166.2	166.2	166.2	166.2
$I_{SC}(A)$	20.8	20.8	20.8	20.8	20.8	20.8	20.8	20.8
$V_m(V)$	137.7	138	138.8	138.5	138.5	138.5	138.5	139.3
$I_m(A)$	14.48	14.57	14.67	14.86	14.86	14.86	14.86	15.13
$P_{GMPP}(W)$	1994	2010	2037	2059	2059	2059	2059	2108
$P_{LMPP}(W)$	1353	1331	1292	1274	1274	1274	1274	1729
$PL(W)$	616	600	573	551	551	551	551	502
FF	0.5768	0.5816	0.589	0.5954	0.5954	0.5954	0.5954	0.6097
$V_{OC}(V)$	166.2	166.2	166.2	166.2	166.2	166.2	166.2	166.2
$I_{SC}(A)$	20.8	20.8	20.8	20.8	20.8	20.8	20.8	18.2
$V_m(V)$	138.2	138.7	138.2	139	139	139	139	136
$I_m(A)$	12.2	12.4	12.32	12.4	12.4	12.4	12.4	14.73
$P_{GMPP}(W)$	1686	1721	1703	1725	1725	1725	1725	2004
$P_{LMPP}(W)$	1307	1274	1292	1274	1274	1274	1274	1097
$PL(W)$	924	889	907	885	885	885	885	606
FF	0.4877	0.4975	0.4925	0.4986	0.4986	0.4986	0.4986	0.6623
Performance Parameters	**Case-3**							
	SP	BL	HC	TCT	BL-HC	BL-TCT	SP-TCT	LS-TCT
$V_{OC}(V)$	160.7	160.7	160.7	160.7	160.7	160.7	160.7	166
$I_{SC}(A)$	20.8	20.8	20.8	20.8	20.8	20.8	20.8	15.6
$V_m(V)$	138.6	138.6	138.6	138.6	138.6	138.6	138.6	131.9
$I_m(A)$	9.949	9.949	9.949	9.949	9.949	9.949	9.949	14.35
$P_{GMPP}(W)$	1379	1379	1379	1379	1379	1379	1379	1892
$P_{LMPP}(W)$	1274	1274	1274	1274	1274	1274	1274	0
$PL(W)$	1231	1231	1231	1231	1231	1231	1231	718
FF	0.4125	0.4125	0.4125	0.4125	0.4125	0.4125	0.4125	0.7309

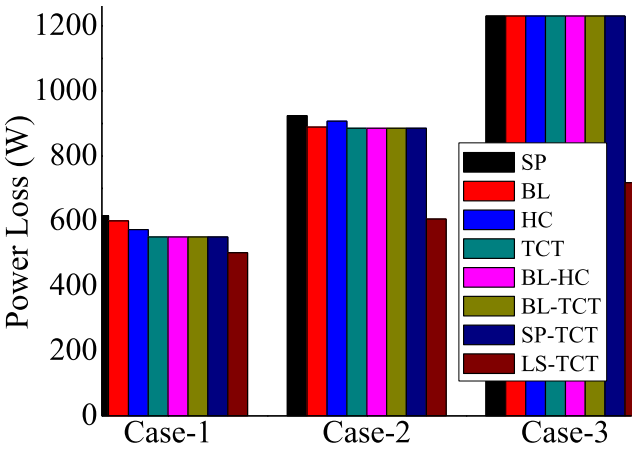

FIGURE 15. Power losses for cases 1-3 under shading pattern-2.

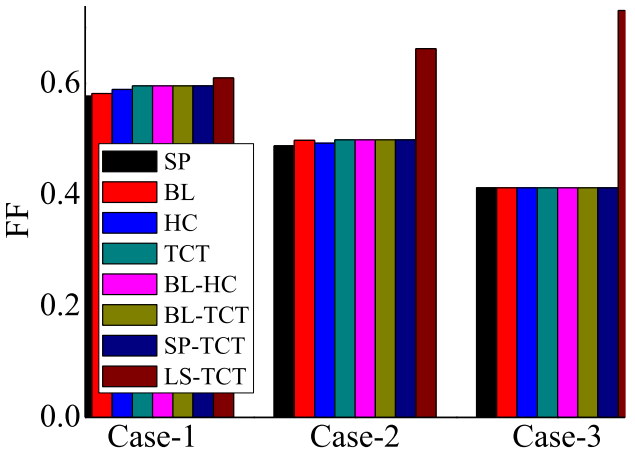

FIGURE 16. Fill factor for cases 1-3 under shading pattern-2.

2) POWER LOSS

In each case of shading pattern-2, the LS-TCT puzzle pattern unveils better performance in comparison to all eight 4 × 4 interconnected topologies. The power losses are expressed using bar graph by Fig. 15, and through tabular form presented in Table 3 respectively. Power losses are found to be lower in the LS-TCT puzzle pattern under all the shading conditions.

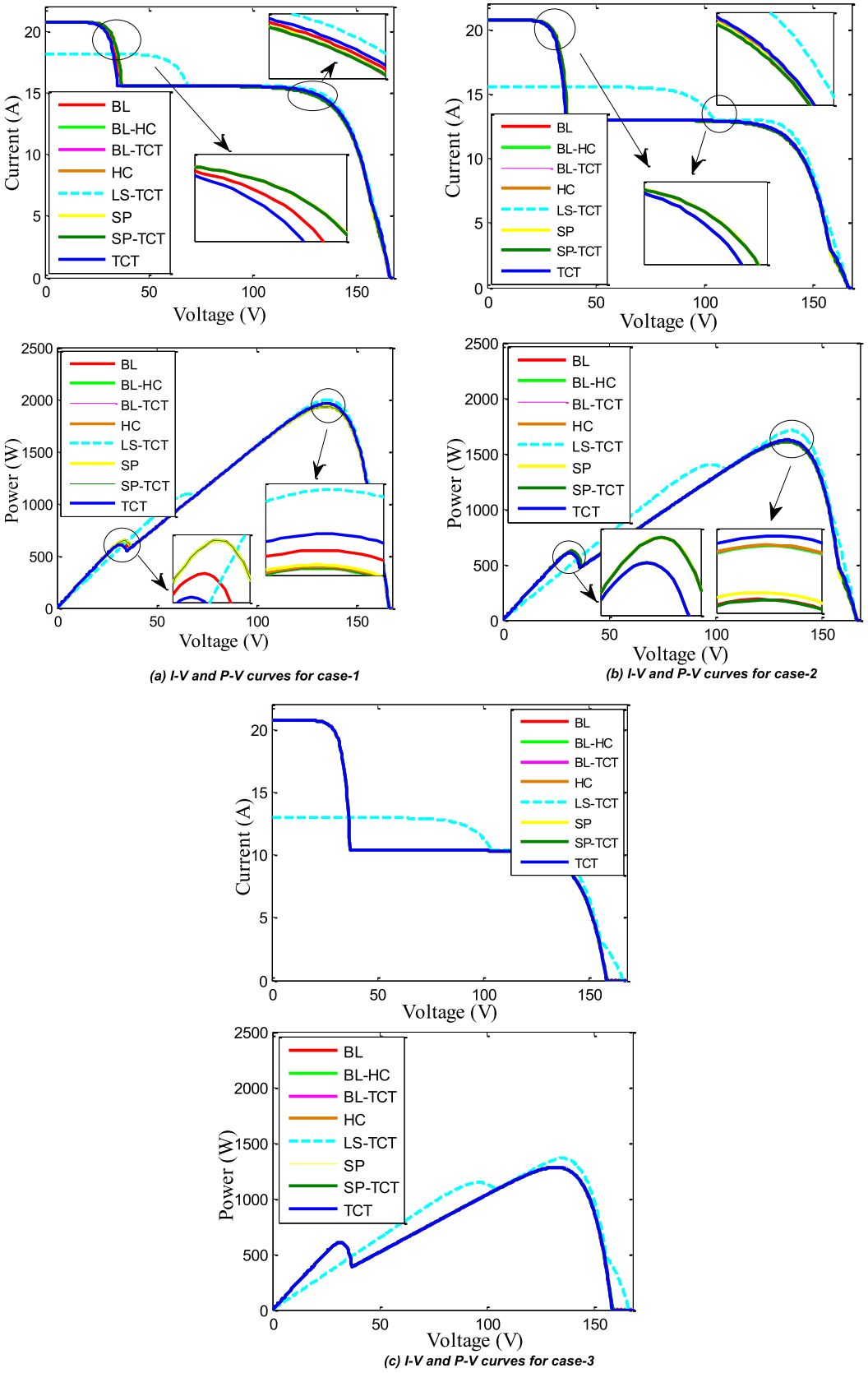

FIGURE 17. (a)-(c). I-V and P-V curves under shading pattern-2.

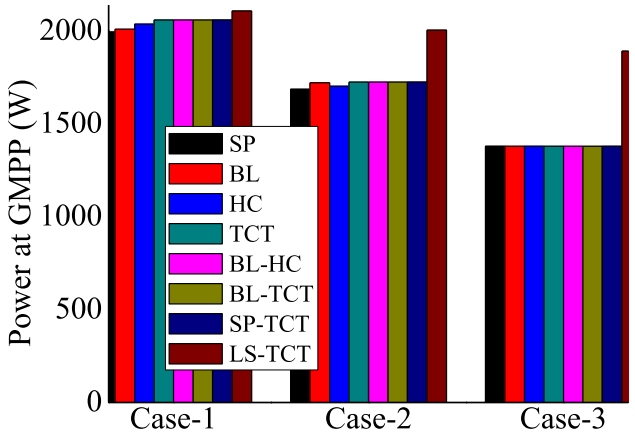

FIGURE 18. Power at GMPP for cases 1-3 under shading pattern-3.

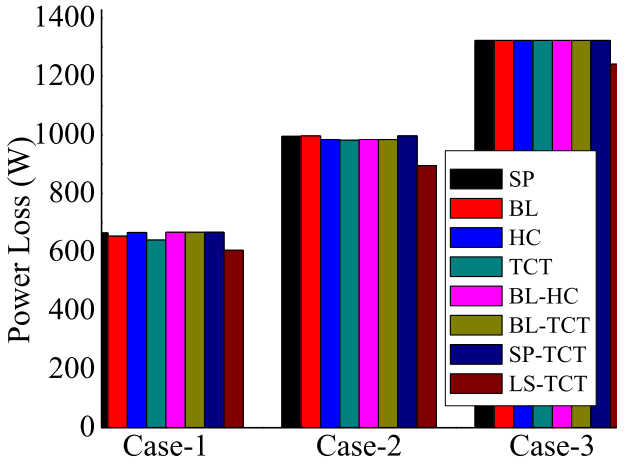

FIGURE 19. Power losses for cases 1-3 under shading pattern-3.

3) FILL FACTOR

The effect of shade gets escalated with its movement from one end to another on the PV Array resulting in a decrease in FF. Through the cases of pattern-2 shown in Fig. 6 (a)-(c), it is constituted as a bar graph and presented through Fig. 16. The values corresponding to it are represented in Table 3 for all the configurations considered in shading pattern-1. It is clearly inferred that FF for LS-TCT topology is superior for the shading pattern-2.

D. EFFECT ON PV ARRAY CONFIGURATIONS UNDER SHADING PATTERN-3

1) P-V AND I-V CURVES

In cases '1-3' of shading pattern- 3, the P–V curves are presented in Fig. 17 of the PV array. On the P–V plot, various MPP's are observed with reference to the shading instance represented through Fig. 7(a) - (c). It has been inferred from the graph that local and global MPP are far apart from each other. It is observed in the shading instance referred to Fig. 7(a) that the effect of shading gets escalated as we move on from cases '1-3'on the power curve. The power demonstrated at GMPP is 1945 W, 1956 W, 1943 W, 1969 W, 1942 W, 1942 W, 1942 W, and 2004 W for SP, BL, HC, TCT, BL-HC, BL–TCT, SP–TCT, and LS-TCT framework respectively. For the shading instance of Fig. 7(b), the P–V curve is presented in Fig. 17(b). It has been inferred through the graph that local and global MPP are far apart from one another. The power observed at GMPP is 1615 W, 1613 W, 1626 W, 1628 W, 1626 W, 1626 W, 1613 W, and 1715 W for SP, BL, HC, TCT, BL-HC, BL–TCT, SP–TCT, and LS-TCT arrangement. For the shading instance of Fig. 7(c), the P–V plot is revealed in Fig. 17(c). The power observed at GMPP for this case is 1287 W, 1287 W, 1287 W, 1287 W, 1287 W, 1287 W, 1287 W, and 1368 W for SP, BL, HC, TCT, BL-HC, BL–TCT, SP–TCT and LS-TCT interconnection respectively as shown in Fig. 18 with bar graph representation.

The electrical performance parameters such as current, voltage, and power of LS-TCT arrangement are shown in Table 4. The PV array power generated is escalated in few cases considering distinct shading scenarios after the reordering of a unit (modules) in accordance with LS puzzle pattern.

2) POWER LOSS

In each case of shading pattern-3, the LS-TCT puzzle pattern unveils better efficacy among all interconnected topologies. The power losses are expressed using the bar graph presented by Fig. 19 and through Table 10 respectively. In addition, the power loss parameters is found to be least in the LS-TCT puzzle pattern under all shading conditions for pattern-3.

3) FILL FACTOR

The effect of shadow gets escalated with its movement from one end to another on the PV Array resulting in a decrease in FF. Through the three shading instances of shading pattern-3 in Fig. 7 (a)-(c), it is constituted as a bar graph and is presented through Fig. 20. The values corresponding to it are represented in Table 4 for all the configurations considered in shading pattern-3. It is clearly inferred that FF for LS-TCT topology is superior for the shading pattern-3.

E. RESULTS VALIDATION

1) ANALYSIS OF SHADING PATTERN-4

Under shading pattern-4, a comprehensive investigation to validate the performance of 4×4 sizes TCT, LS-TCT, SDK, and SPDK configurations is considered. This shading scenario is comprised of two realistic shading cases with irradiation levels such as $1000W/m^2$, $500W/m^2$ and $300W/m^2$ that are considered during the study, as shown in Fig. 21.

2) MATLAB/SIMULINK ANALYSIS: P-V AND I-V CHARACTERISTICS

A thorough comparative study of the achieved performance of 4×4 sizes of TCT, SDK, and SPDK configurations is being

TABLE 4. Current, voltage, power, PL, mismatch power loss and FF for configuration experiencing shading pattern-3.

Performance Parameters	Case-1							
	SP	BL	HC	TCT	BL-HC	BL-TCT	SP-TCT	LS-TCT
$V_{OC}(V)$	166	166	166	166	166	166	166	166
$I_{SC}(A)$	20.8	20.8	20.8	20.8	20.8	20.8	20.8	18.2
$V_m(V)$	134.7	135.2	134.8	135.4	134.8	134.8	134.8	135.3
$I_m(A)$	14.44	14.47	14.42	14.55	14.41	14.41	14.41	14.81
$P_{GMPP}(W)$	1945	1956	1943	1969	1942	1942	1942	2004
$P_{LMPP}(W)$	645.7	622.8	645.7	606.6	645.7	645.7	645.7	1097
$PL(W)$	665	654	667	641	668	668	668	606
FF	0.5633	0.5666	0.563	0.5706	0.5626	0.5626	0.5626	0.6632
$V_{OC}(V)$	165.8	165.8	165.8	165.8	165.8	165.8	165.8	165.8
$I_{SC}(A)$	20.8	20.8	20.8	20.8	20.8	20.8	20.8	15.6
$V_m(V)$	133.7	133.8	134.1	134.1	134	134	133.9	136
$I_m(A)$	12.08	12.06	12.13	12.14	12.13	12.13	12.05	12.61
$P_{GMPP}(W)$	1615	1613	1626	1628	1626	1626	1613	1715
$P_{LMPP}(W)$	622.8	622.8	606.6	606.6	606.6	606.6	622.8	1407
$PL(W)$	995	997	984	982	984	984	997	895
FF	0.4683	0.4679	0.4717	0.4721	0.4713	0.4713	0.4679	0.663
Performance Parameters	**Case-3**							
	SP	**BL**	**HC**	**TCT**	**BL-HC**	**BL-TCT**	**SP-TCT**	**LS-TCT**
$V_{OC}(V)$	158.3	158.3	158.3	158.3	158.3	158.3	158.3	165.7
$I_{SC}(A)$	20.08	20.08	20.08	20.08	20.08	20.08	20.08	13
$V_m(V)$	132.5	132.5	132.5	132.5	132.5	132.5	132.5	135.4
$I_m(A)$	9.713	9.713	9.713	9.713	9.713	9.713	9.713	10.1
$P_{GMPP}(W)$	1287	1287	1287	1287	1287	1287	1287	1368
$P_{LMPP}(W)$	605.9	605.9	605.9	605.9	605.9	605.9	605.9	1148
$PL(W)$	1323	1323	1323	1323	1323	1323	1323	1242
FF	0.4049	0.4049	0.4049	0.4049	0.4049	0.4049	0.4049	0.6349

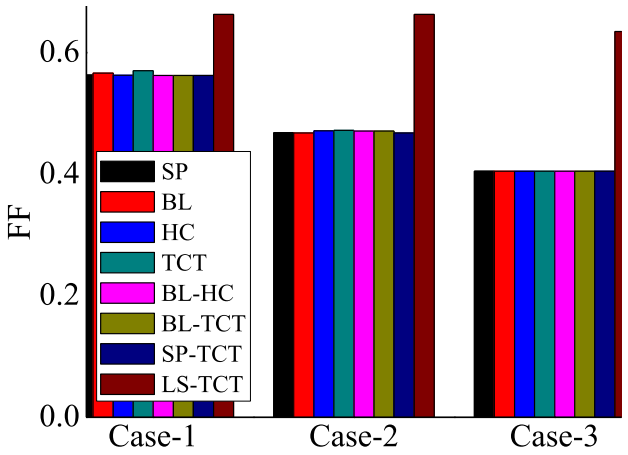

FIGURE 20. FF for cases 1-3 under shading pattern-3.

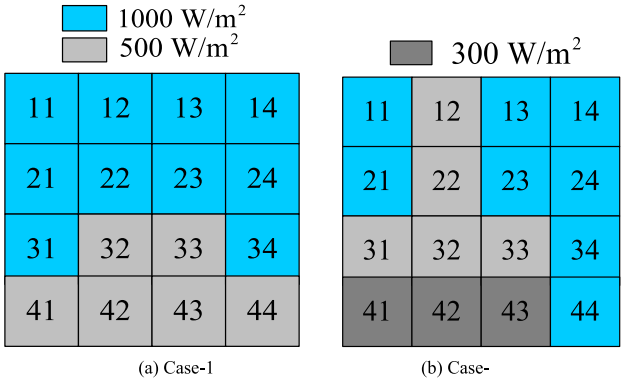

FIGURE 21. (a)-(c). Shading cases 1-3 for pattern-4.

considered. The MPP is located at 80W in ideal conditions. The behaviour of the obtained P-V curves for the regarded PV array connections is examined under two shading scenarios (pattern-4) and is depicted in Fig. 22(a)-(b).

The TCT configuration suffered significant power losses due to a lack of cohesiveness between the PV module power maxima and array's GMPP. Under two non-uniform irradiance levels (1000W/m^2 and 500W/m^2), the GMPP of the TCT configuration is 47.08W in shading case-I. Furthermore,

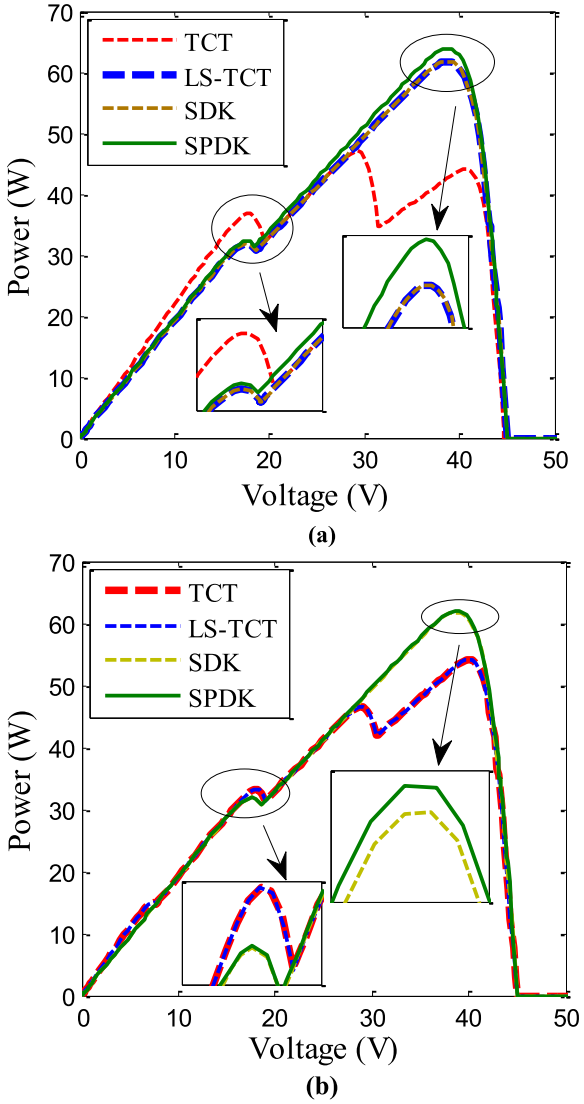

FIGURE 22. (a)-(b). P-V characteristics of TCT, LS-TCT, SDK and SPDK configurations during MATLAB/Simulation.

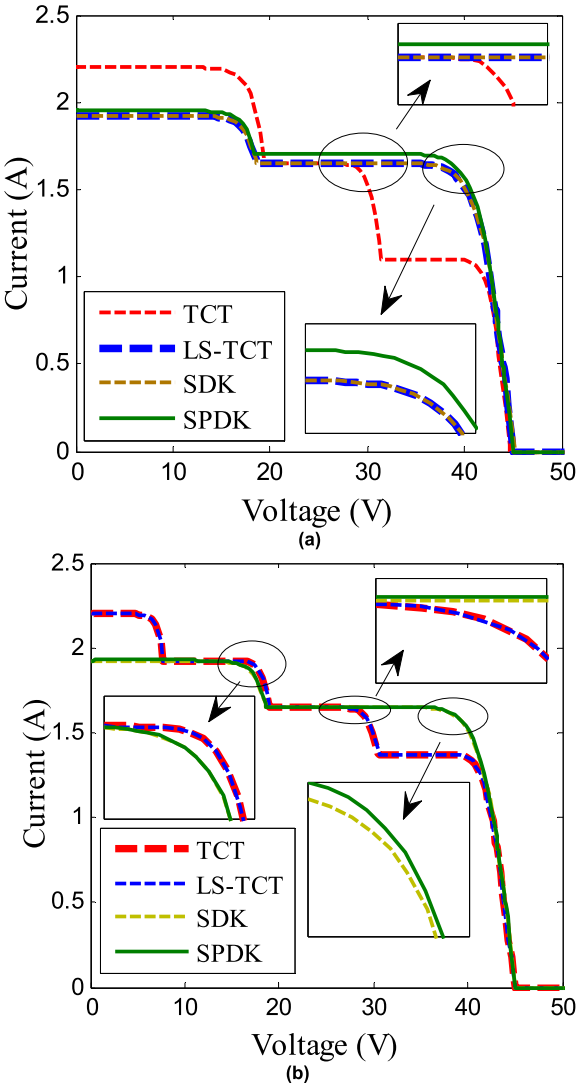

FIGURE 23. (a)-(b). I-V characteristics of TCT, LS-TCT, SDK and SPDK configurations during MATLAB/Simulation.

under similar sun irradiance conditions, LS-TCT, SDK, and SPDK configurations are investigated, and GMPP locations are observed to be 61.77W, 61.77W, and 63.89W, respectively. The performance output of the PV array configurations under consideration is investigated based on the highest GMPP and the fewest number of power maxima on P-V curves under PSCs.

During a similar shading case-II, the highest power losses are observed to be 25.86W in TCT and LS-TCT configurations, with the lowest equal GMPP values being 54.14W. The GMMP locations for SDK and SPDK configurations are 61.81W and 61.95W, respectively. Overall, in the shading case-I study, SPDK has the best GMPP and the lowest power losses (18.05W), as well as an improved FF (0.714).

As shown in Fig. 23(a), the I-V characteristics of TCT, LS-TCT, SDK and SPDK configurations are tested under shading case-I (pattern-4). The highest maximum current (I_m) observed for SPDK configuration is 1.652A compared to TCT, LS-TCT, and SDK configurations of 1.611A, 1.582A, and 1.582A, respectively. The open circuit voltage (V_{OC}) values are 44.64V, 45.028V, 45.028V, and 45.028V, respectively.

For shading case-II (pattern-4), the values of I_m are 1.351A, 1.351A, 1.589A, and 1.350A for TCT, LS-TCT, SDK, and SPDK configurations, respectively. V_{OC} values are observed to be 45.028V for all PV array configurations. It demonstrates that non-uniformity sun irradiance is more harmful to short circuit current than V_{OC}.

3) EXPERIMENTAL ANALYSIS: P-V AND I-V CHARACTERISTICS

An experimental study on 4 × 4 size of TCT, LS-TCT, SDK and SPDK configurations is performed. Under ideal/uniform irradiance such as 1000W/m^2, MPP is observed as 80W. The present study on PV system configurations is deliberated under similar shading cases I-II (pattern-4). Fig. 24 shows

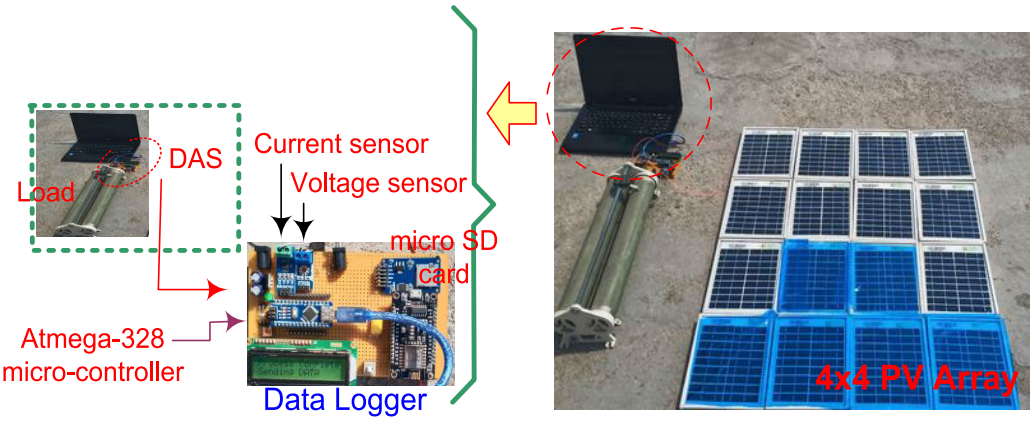

FIGURE 24. Experimental setup of PV system.

TABLE 5. Specifications of 5W PV module at standard test conditions.

Parameters	Values
P_m	5W
V_m	9.62V
I_m	0.52A
V_{OC}	11.25V
I_{SC}	0.55A

the experimental setup and the major components of are as follows (i) sixteen PV modules arranged in 4 × 4 matrix (ii) resistive load (variable) and (iii) self-developed data logger to store real time voltage, current data to characterize PV system. This data logger system was developed with voltage and current sensors to measure real-time electrical data during experimentation. The open source Arduino System (ATmega-328 micro-controller) operated the system performance. The real time electrical data is stored in micro SD card for further investigation. Table-5 shows the specifications of commercially available solar PV modules used for MATLAB/Simulink modeling and experimental studies.

An extensive experimental study is performed and obtained electrical performance of TCT, LS-TCT, SDK and SPDK configurations is deliberated. The P-V curves for all four PV array configurations are obtained under shading cases I-II, shown in Fig. 25(a)-(b).

The TCT configuration is experiencing a large amount of shading losses due to lack of coherence between the power maxima point of PV modules in an array. In shading case-I, the GMPP of the TCT configuration is 45.77W at non-uniform irradiation levels such as 1000W/m^2 and 500W/m^2. In addition, the GMPPs are found as 59.95W, 59.95W and 62.25W for LS-TCT, SDK and SPDK configurations respectively. The performance of SPDK is having best performance compared to all among PV configurations under PSCs.

Furthermore, it is observed that the TCT configuration has low value of GMPP as 52.62W under non-uniform irradiation levels such as 1000W/m^2, 500W/m^2, and 300W/m^2. Under similar shading scenarios, LS-TCT, SDK and SPDK configurations are having different GMPP locations as 54.69W, 60.55W and 61.96W respectively.

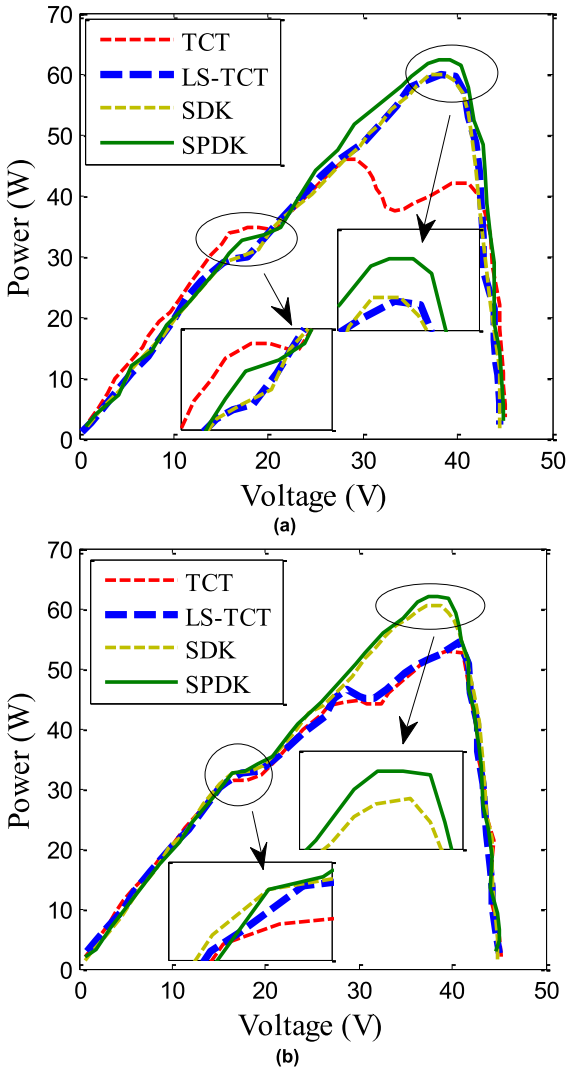

FIGURE 25. (a)-(b). P-V characteristics of TCT, LS-TCT, SDK and SPDK configurations during experimental study.

The irradiation level affects the short circuit current of PV system. During the non-uniform irradiations,

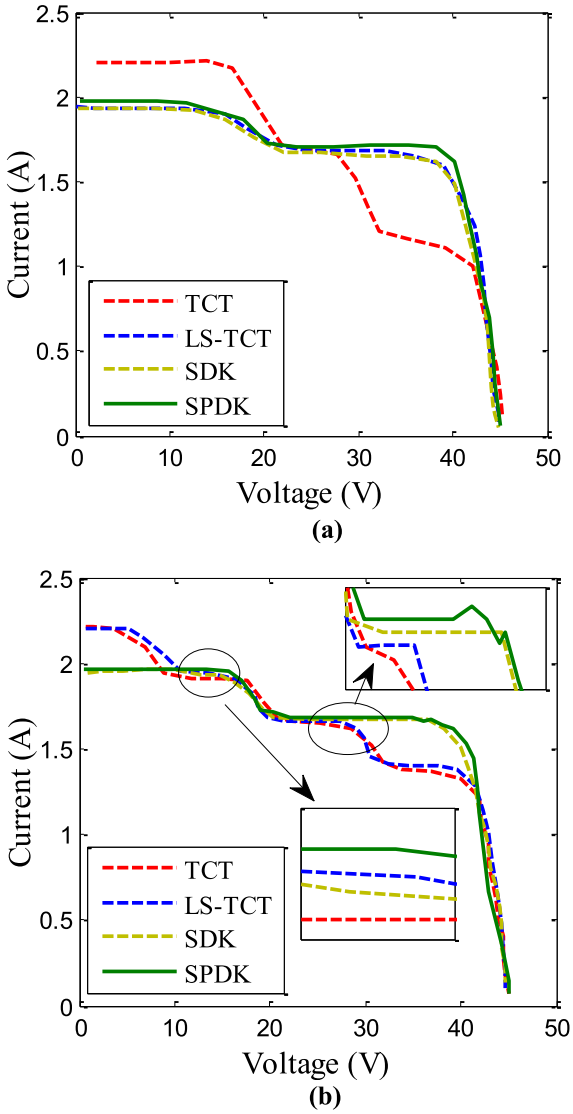

FIGURE 26. (a)-(b). I-V characteristics of TCT, LS-TCT, SDK and SPDK configurations during experimental study.

I-V characteristics of TCT, LS-TCT, SDK and SPDK configurations are shown in Fig. 26(a)-(b). For shading case-I (pattern-4), short circuit current values are observed as 2.202A, 1.927A, 1.927A and 1.927A for TCT, LS-TCT, SDK and SPDK configurations respectively. The value of FF is investigated as 0.708, 0.801, 0.801 and 0.807 respectively, SPDK configuration has best performance under distinguish shading scenarios such as 1000W/m^2 and 500W/m^2.

Under shading case-II, the irradiation levels are considered as 1000W/m^2, 500W/m^2 and 300W/m^2 for performance investigations. The short circuit current values are observed as 2.22A, 2.22A, 1.955A and 1.968A for TCT, LS-TCT, SDK, and SPDK configurations due to shading effect. In addition this, the value of FF is investigated as 0.526, 0.551, 0.6873 and 0.6982 respectively, SPDK configuration has best performance under distinguish shading scenarios.

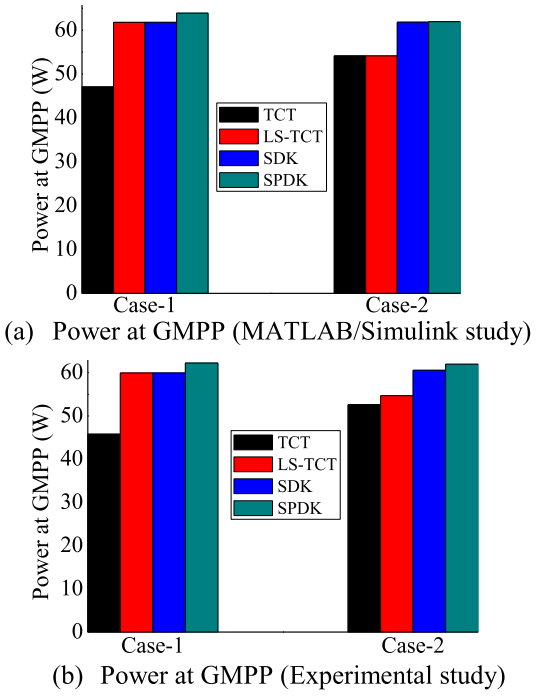

FIGURE 27. (a) Power at GMPP during MATLAB/Simulink Study (b) Power at GMPP during experimental study.

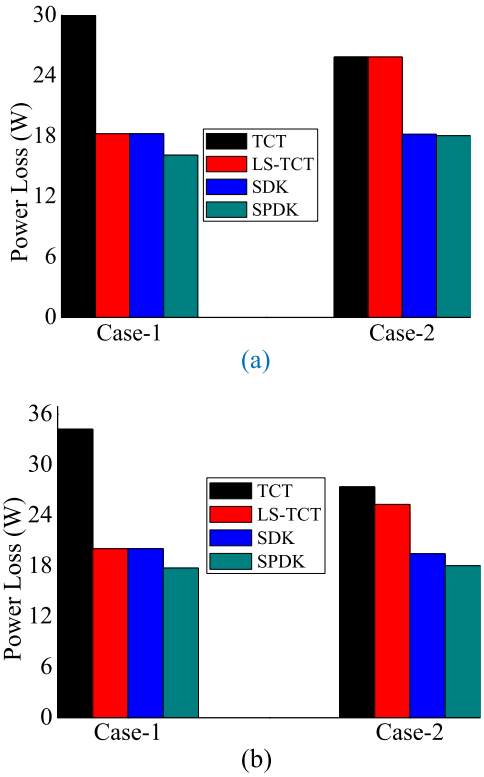

FIGURE 28. (a) PL during MATLAB/Simulink Study (b) PL during experimental study.

4) POWER AT GMPP

The GMMP location is investigated and depicted in figure 27(a)-(b) for MATLAB/Simulink and experimental

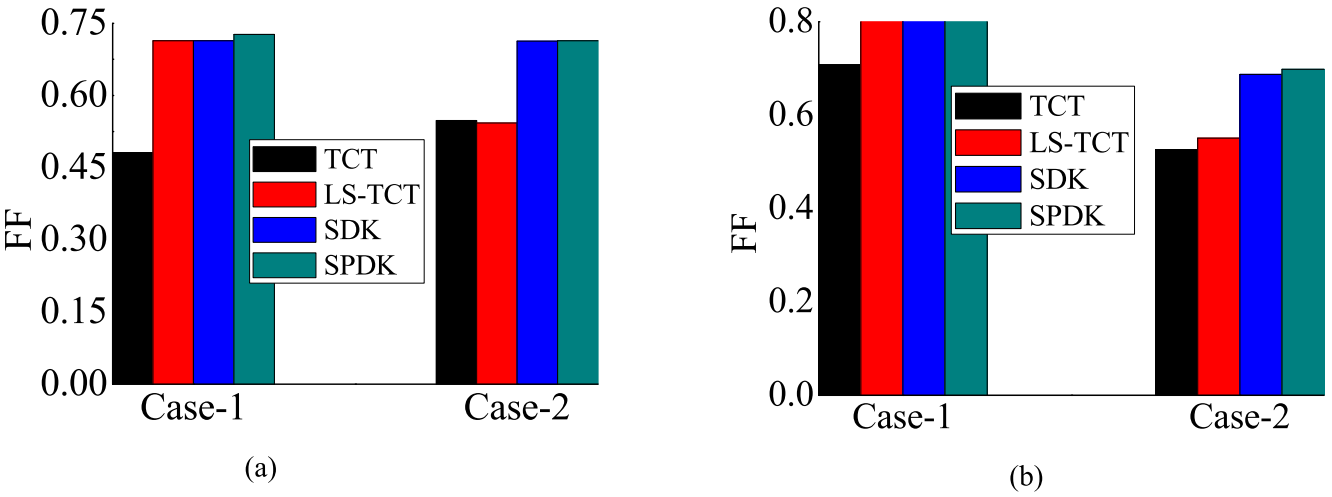

FIGURE 29. (a) FF during MATLAB/Simulink Study (b) FF during experimental study.

TABLE 6. Current, voltage, power, PL, mismatch power loss and FF configuration experiencing shading pattern-4.

Performance Parameters	Case-1							
	MATLAB/Simulation study				Experimental study			
	TCT	**LS-TCT**	**SDK**	**SPDK**	**TCT**	**LS-TCT**	**SDK**	**SPDK**
$V_{OC}(V)$	44.64	45.028	45.028	45.028	44.88	44.45	44.18	44.65
$I_{SC}(A)$	2.19	1.92	1.92	1.95	2.202	1.927	1.927	1.977
$V_m(V)$	29.22	39.03	39.03	38.66	29.32	38.54	38.54	39.29
$I_m(A)$	1.611	1.582	1.582	1.652	1.561	1.555	1.555	1.584
$P_{GMPP}(W)$	47.08	61.77	61.77	63.89	45.77	59.95	59.95	62.25
$P_{LMPP}(W)$	36.68	31.86	31.86	32.34	34.8	29.99	29.99	32.51
$PL(W)$	32.92	18.23	18.23	16.11	34.23	20.05	20.05	17.75
FF	0.481	0.714	0.714	0.727	0.708	0.801	0.801	0.807
Performance Parameters	**Case-2**							
	MATLAB/Simulation study				Experimental study			
	TCT	**LS-TCT**	**SDK**	**SPDK**	**TCT**	**LS-TCT**	**SDK**	**SPDK**
$V_{OC}(V)$	45.028	45.028	45.028	45.028	45.03	45.04	45.06	45.09
$I_{SC}(A)$	2.199	2.199	1.924	1.927	2.22	2.22	1.955	1.968
$V_m(V)$	40.05	40.05	38.89	38.97	41.11	41.04	38.77	38.47
$I_m(A)$	1.351	1.351	1.589	1.350	1.279	1.330	1.561	1.610
$P_{GMPP}(W)$	54.14	54.14	61.81	61.95	52.62	54.69	60.55	61.96
$P_{LMPP}(W)$	33.26	33.26	31.9	31.9	31.24	32.49	32.49	32.49
$PL(W)$	25.86	25.86	18.19	18.05	27.38	25.31	19.45	18.04
FF	0.548	0.543	0.713	0.714	0.526	0.551	0.6873	0.6982

study. In MATLAB/Simulink study, higher GMPP locations are observed as 63.89W and 61.95W for SPDK configuration compared to TCT, LS-TCT and SDK configurations during shading cases I-II (pattern-4) respectively.

In addition, highest power at GMPP is assessed as 62.25W and 61.95W for SPDK configurations compared to TCT, LS-TCT and SDK configurations during shading cases I-II (pattern-4) respectively during experimentation work.

5) POWER LOSS

Calculation of PL are carried out under shading case I-II (pattern-4). The obtained results are depicted in Fig. 28(a)-(b) for MATLAB/Simulink and experimentation work. The highest and lowest shading case-I is experienced by TCT and SPDK configurations as 32.92W and 16.11W respectively compared to LS-TCT and SDK configurations. Moreover, minimized power PL is found as 18.05W for SPDK configuration compared to TCT, LS-TCT and SDK.

TABLE 7. Comparative study among with and without bypass diode connected system of TCT interconnection.

Parameters	TCT scheme without BPD	TCT scheme with BPD
$P_{Generated}(W)$	45.98	59.56
$V_{Array}(V)$	42.55	29.10
$I_{Array}(A)$	1.08	2.04
Number of peaks	1	2

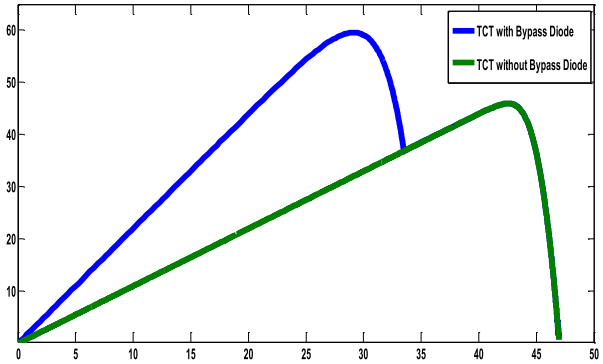

(a)

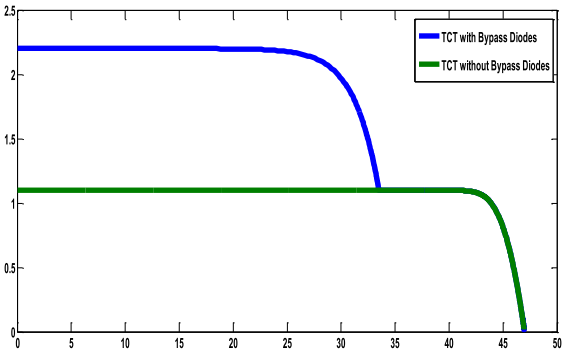

(b)

FIGURE 30. (a) Characteristics of a TCT connected system under PSCs via with and without bypass diode (a) P-V curves (b) I-V curves.

Under experimentation work, the minimized PL are observed during shading case I-II are experienced for SPDK configuration as 16.11W and 18.05W respectively compared to LS-TCT and SDK configurations.

6) FILL FACTOR

FF assessment with dissimilarities observation found due to shading cases I-II (pattern-4) for the TCT, LS-TCT, SDK and SPDK configurations and statistically represented in figure 29. During MATLAB/Simulink study, SPDK has improved value of FF as 0.727 and 0.714 respectively. Moreover, the investigation of FF is carried out and observed highest as 0.806 and 0.698 during experimental study under similar shading cases I-II respectively.

Critical study on shading effect analysis on PV system is performed and all the quantitative outcomes are summarized in Table-5 as,

F. EFFECT OF BYPASS DIODE ON PV ARRAY

The bypass diode (BPD) plays a huge role in power generation of a PV array. During the PSCs without bypass diode, the PV array carries a current of shaded modules generated current. As per the property of series connection, the series connected PV array produces less amount of current, due to this power generation capacity of PV array greatly reduces. On the other side, the bypass diode acts as additional path for the current flow in-case of a shaded condition. Thereby shaded PV modules current is by passed and remaining PV array in a position to carry actual current produced by un-shaded PV module. Due to this there exist two different levels of current in a Bypass diode connected system. Thereby it results multiple peaks in a PV array. However the system exhibits multiple peaks power generated capacity of a PV array will be high than without bypass diode connected system. To confirm the same, by considering the same PV modules, shading of TCT connected system, authors performed simulation under two different conditions and obtained results are table in Table to show clear understand on the impact of bypass diode over TCT connected PV system. From the table it can be observe that, there is less differ of power between those, however, if we implement the same to high rated system, different will be huge and it shows significant improve in power generation than without bypass diode connected system. In addition, the I-V and P-V characteristics have been plotted to shows its effect pictorially in Fig. 30(a)-(b). The quantitative values are depicted in Table-6.

V. CONCLUSION

This paper successfully investigated the performance of SP, BL, HC, BL-HC, TCT, SP–TCT, BL–TCT, and LS-TCT configurations using the MATLAB/Simulink models. The performance has been assessed by current, voltage, power at GMPP, FF, and PL. Due to dispersion in shading, LS-TCT configuration exhibited the lowest PL and increased FF values among eight electrical arrangements.

- The puzzle-based LS-TCT configurations are more productive leading to utmost PE of 8.4 %, power mismatch losses get reduced to 867W, and FF gets maximally escalated by 0.037 under shading pattern-1.
- The production of LS-TCT configuration has utmost PE by 27.11%, maximum redundancy in mismatch power by 1787 W, incremented FF by 0.32 compared to TCT (which has higher performance among all configurations, except LS-TCT) is observed for shading pattern-2.

- It has been acclaimed for the suggested puzzle-based configuration that the extracted output power is higher when study performed under PSCs.
- Proposed SPDK puzzle based PV array configurations has best performance e.g. GMPP, PL and FF 63.89W, 16.11W, 0.727 (MATLAB/Study) and 62.25W, 17.75W, 0.807 (experimental study) respectively under shading cases-1 (pattern-4).
- Experimental study is performed to validate the PV system performance, which also proved the direction of implementation at commercial level under such shading scenarios.

REFERENCES

[1] M. Premkumar, U. Subramaniam, T. S. Babu, R. M. Elavarasan, and L. Mihet-Popa, "Evaluation of mathematical model to characterize the performance of conventional and hybrid PV array topologies under static and dynamic shading patterns," *Energies*, vol. 13, no. 12, pp. 1–37, 2020.

[2] D. Yousri, T. S. Babu, S. Mirjalili, N. Rajasekar, and M. A. Elaziz, "A novel objective function with artificial ecosystem-based optimization for relieving the mismatching power loss of large-scale photovoltaic array," *Energy Convers. Manage.*, vol. 225, Dec. 2020, Art. no. 113385.

[3] G. Petrone and C. A. Ramos-Paja, "Modeling of photovoltaic fields in mismatched conditions for energy yield evaluations," *Electr. Power Syst. Res.*, vol. 81, no. 4, pp. 1003–1013, Apr. 2011.

[4] Y. J. Wang and P.-C. Hsu, "Analytical modelling of partial shading and different orientation of photovoltaic modules," *IET Renew. Power Gener.*, vol. 4, no. 3, pp. 272–282, May 2010.

[5] B. I. Rani, G. S. Ilango, and C. Nagamani, "Enhanced power generation from PV array under partial shading conditions by shade dispersion using Su-Do-Ku configuration," *IEEE Trans. Sustain. Energy*, vol. 4, no. 3, pp. 594–601, Jul. 2013.

[6] L. Fialho, R. Melicio, V. M. F. Mendes, J. Figueiredo, and M. Collares-Pereira, "Effect of shading on series solar modules: Simulation and experimental results," *Procedia Technol.*, vol. 17, pp. 295–302, Jan. 2014.

[7] K. S. Koray, "FPGA based new MPPT method for PV array system operating partially shaded conditions," *Energy*, vol. 68, pp. 399–410, Apr. 2014.

[8] S. Moballegh and J. Jiang, "Modeling, prediction, and experimental validations of power peaks of PV arrays under partial shading conditions," *IEEE Trans. Sustain. Energy*, vol. 5, no. 1, pp. 293–300, Jan. 2014.

[9] S. Pareek and R. Dahiya, "Output power maximization of partially shaded 4×4 PV field by altering its topology," *Energy Procedia*, vol. 54, pp. 116–126, Jan. 2014.

[10] J. Qi, Y. Zhang, and Y. Chen, "Modeling and maximum power point tracking (MPPT) method for PV array under partial shade conditions," *Renew. Energy*, vol. 66, pp. 337–345, Jun. 2014.

[11] R. Ramaprabha, "Selection of an optimum configuration of solar PV array under partial shaded condition using particle swarm optimization," *Int. J. Elect. Comput. Eng.*, vol. 8, no. 1, pp. 96–103, 2014.

[12] S. Vijayalekshmy, S. R. Iyer, and B. Beevi, "Comparative analysis on the performance of a short string of series-connected and parallel-connected photovoltaic array under partial shading," *J. Inst. Eng., B*, vol. 96, no. 3, pp. 217–226, Sep. 2015.

[13] J. Bai, Y. Cao, Y. Hao, Z. Zhang, S. Liu, and F. Cao, "Characteristic output of PV systems under partial shading or mismatch conditions," *Sol. Energy*, vol. 112, pp. 41–54, Feb. 2015.

[14] S. N. Deshkar, S. B. Dhale, J. S. Mukherjee, T. S. Babu, and N. Rajasekar, "Solar PV array reconfiguration under partial shading conditions for maximum power extraction using genetic algorithm," *Renew. Sustain. Energy Rev.*, vol. 43, pp. 102–110, Mar. 2015.

[15] S. Malathy and R. Ramaprabha, "Comprehensive analysis on the role of array size and configuration on energy yield of photovoltaic systems under shaded conditions," *Renew. Sustain. Energy Rev.*, vol. 49, pp. 672–679, Sep. 2015.

[16] P. S. Rao, P. Dinesh, G. S. Ilango, and C. Nagamani, "Optimal Su-Do-Ku based interconnection scheme for increased power output from PV array under partial shading conditions," *Frontiers Energy*, vol. 9, no. 2, pp. 199–210, Jun. 2015.

[17] S. Vijayalekshmy, G. R. Bindu, and S. R. Iyer, "Analysis of various photovoltaic array configurations under shade dispersion by Su Do Ku arrangement during passing cloud conditions," *Indian J. Sci. Technol.*, vol. 8, no. 35, pp. 1–7, Dec. 2015.

[18] S. Vijayalekshmy, G. R. Bindu, and S. R. Iyer, "Performance improvement of partially shaded photovoltaic arrays under moving shadow conditions through shade dispersion," *J. Inst. Eng. B*, vol. 97, no. 4, pp. 1–7, 2015.

[19] A. S. Yadav, R. K. Pachauri, and Y. K. Chauhan, "Comprehensive investigation of PV arrays under different shading patterns by shade dispersion using puzzled pattern based Su-Do-Ku puzzle configuration," in *Proc. 1st Int. Conf. Next Gener. Comput. Technol. (NGCT)*, Sep. 2015, pp. 824–830.

[20] H. S. Sahu and S. K. Nayak, "Extraction of maximum power from a PV array under nonuniform irradiation conditions," *IEEE Trans. Electron Devices*, vol. 63, no. 12, pp. 4825–4831, Dec. 2016.

[21] H. S. Sahu, S. K. Nayak, and S. Mishra, "Maximizing the power generation of a partially shaded PV array," *IEEE J. Emerg. Sel. Topics Power Electron.*, vol. 4, no. 2, pp. 626–637, Jun. 2016.

[22] S. Pareek, N. Chaturvedi, and R. Dahiya, "Optimal interconnections to address partial shading losses in solar photovoltaic arrays," *Sol. Energy*, vol. 155, pp. 537–551, Oct. 2017.

[23] N. Mishra, A. S. Yadav, R. Pachauri, Y. K. Chauhan, and V. K. Yadav, "Performance enhancement of PV system using proposed array topologies under various shadow patterns," *Sol. Energy*, vol. 157, pp. 641–656, Nov. 2017.

[24] S. Malathy and R. Ramaprabha, "Reconfiguration strategies to extract maximum power from photovoltaic array under partially shaded conditions," *Renew. Sustain. Energy Rev.*, vol. 81, pp. 2922–2934, Jan. 2018.

[25] R. K. Pachauri, A. S. Yadav, Y. K. Chauhan, A. Sharma, and V. Kumar, "Shade dispersion based photovoltaic array configurations for performance enhancement under partial shading conditions," *Int. Trans. Electr. Energy Syst.*, vol. 28, no. 7, pp. 1–32, 2018.

[26] G. S. Krishna and T. Moger, "Improved Su-Do-Ku reconfiguration technique for total-cross-tied PV array to enhance maximum power under partial shading conditions," *Renew. Sustain. Energy Rev.*, vol. 109, pp. 333–348, Jul. 2019.

[27] I. Nasiruddin, S. Khatoon, M. F. Jalil, and R. C. Bansal, "Shade diffusion of partial shaded PV array by using odd-even structure," *Sol. Energy*, vol. 181, pp. 519–529, Mar. 2019.

[28] M. S. S. Nihanth, J. P. Ram, D. S. Pillai, A. M. Y. M. Ghias, A. Garg, and N. Rajasekar, "Enhanced power production in PV arrays using a new skyscraper puzzle based one-time reconfiguration procedure under partial shade conditions (PSCs)," *Sol. Energy*, vol. 194, pp. 209–224, Dec. 2019.

[29] G. Sagar, D. Pathak, P. Gaur, and V. Jain, "A Su Do Ku puzzle based shade dispersion for maximum power enhancement of partially shaded hybrid bridge-link-total-cross-tied PV array," *Sol. Energy*, vol. 204, pp. 161–180, Jul. 2020.

[30] S. Gul, A. U. Haq, M. Jalal, A. Anjum, and I. U. Khalil, "A unified approach for analysis of faults in different configurations of PV arrays and its impact on power grid," *Energies*, vol. 13, pp. 1–23, Jan. 2020.

[31] T. S. Babu, D. Yousri, and K. Balasubramanian, "Photovoltaic array reconfiguration system for maximizing the harvested power using population-based algorithms," *IEEE Access*, vol. 4, pp. 109608–109624, 2020.

[32] G. Madhusudanam, S. Senthilkumar, I. Anand, and P. Sanjeevkumar, "A shade dispersion scheme using Latin square arrangement to enhance power production in solar photovoltaic array under partial shading conditions," *J. Renew. Sustain. Energy*, vol. 10, pp. 1–14, Oct. 2018.

[33] A. Srinivasan, S. Devakirubakaran, and B. M. Sundaram, "Mitigation of mismatch losses in solar PV system—Two-step reconfiguration approach," *Sol. Energy*, vol. 206, pp. 640–654, Aug. 2020.

[34] H. Rezk, A. Fathy, and M. Aly, "A robust photovoltaic array reconfiguration strategy based on coyote optimization algorithm for enhancing the extracted power under partial shadow condition," *Energy Rep.*, vol. 7, pp. 109–124, Nov. 2021.

[35] R. Venkateswari and N. Rajasekar, "Power enhancement of PV system via physical array reconfiguration based Lo Shu technique," *Energy Convers. Manage.*, vol. 215, pp. 1–22, Jul. 2020.

[36] J. J. Wanko and J. V. Nickell, "Shape-Do-Ku puzzles combine logic and spatial reasoning with an understanding of basic geometric conecpts," *Math. Teacher*, vol. 107, no. 3, pp. 188–194, 2013.

RUPENDRA KUMAR PACHAURI received the B.Tech. degree from UP Technical University (formerly), Lucknow, Uttar Pradesh, India, in 2006, the M.Tech. degree from the Electrical Engineering Department, Faculty of Engineering and Technology, Zakir Husain College of Engineering and Technology, Aligarh Muslim University (AMU), Aligarh, India, in 2009, and the Ph.D. degree in renewable energy from G. B. University, India, in 2016. He is currently working as an Assistant Professor (Selection Grade) with the Department of Electrical and Electronics Engineering, University of Petroleum and Energy Studies (UPES), Dehradun, India. He has published more than 85 research articles in international repute science citation/Scopus indexed journals along with IEEE/Springer conferences. His fields of research interests include solar energy, fuel cell technology, applications of ICT in PV systems, and smart grid operations. He has performed reviews for high prestigious journals, including IEEE TRANSACTIONS ON INDUSTRIAL INFORMATICS, IEEE TRANSACTIONS ON INDUSTRIAL ELECTRONICS, *Renewable Energy*, *International Journal of Electrical Power and Energy Systems*, and *Solar Energy*.

ISHA KANSAL received the B.Tech. degree from Quantum University, Uttarakhand, India, in 2012, and the M.Tech. degree in engineering physics from the University School of Basic and Applied Sciences, Guru Gobind Singh Indraprastha University, Dwarka, New Delhi, India, in 2014. She is currently pursuing the Ph.D. degree in renewable energy with the Department of Electrical and Electronics Engineering, School of Engineering, University of Petroleum and Energy Studies (UPES), Dehradun, Uttarakhand. She worked as an Assistant Professor with the Department of Electrical and Electronics Engineering, (UPES). She has published quality research articles in international reputed indexed journals. Her fields of research interests include solar energy and applications of different optimization techniques used in PV systems.

THANIKANTI SUDHAKAR BABU (Senior Member, IEEE) received the B.Tech. degree from Jawaharlal Nehru Technological University, Anantapur, India, in 2009, the M.Tech. degree in power electronics and industrial drives from Anna University, Chennai, India, in 2011, and the Ph.D. degree from VIT University, Vellore, India, in 2017.

He is currently working as an Associate Professor with the Department of Electrical Engineering, Chaitanya Bharathi Institute of Technology (CBIT), Hyderabad, India. He has completed his Postdoctoral Research Fellowship from the Institute of Power Engineering, Universiti Tenaga Nasional (UNITEN), Malaysia. Before to that, he worked as an Assistant Professor with the School of Electrical Engineering, VIT University. He has published more than 70 research articles in various renowned international journals. His research interests include the design and implementation of solar PV systems, renewable energy resources, power management for hybrid energy systems, storage systems, fuel cell technologies, electric vehicles, and smart grids. He has been acting as an Associate Editor of *IET RPG*, IEEE ACCESS, *ITEES* (Wiley), and *Frontiers in Energy Research*; the Section Editor of *Energy* and *Sustainability* (MDPI Publications); and a reviewer of various reputed journals.

HASSAN HAES ALHELOU (Senior Member, IEEE) is currently a Faculty Member with Tishreen University, Lattakia, Syria. He is with University College Dublin, Ireland. He has participated in more than 15 industrial projects. He has published more than 130 research articles in the high quality peer-reviewed journals and international conferences. His major research interests include power systems, power system dynamics, power system operation and control, dynamic state estimation, frequency control, smart grids, micro-grids, demand response, load shedding, and power system protection. He is included in the 2018 and 2019 Publons list of the top 1% best reviewer and researchers in the field of engineering. He was a recipient of the Outstanding Reviewer Award from *Energy Conversion and Management* journal, in 2016, *ISA Transactions* journal, in 2018, *Applied Energy* journal, in 2019, and many other awards. He was a recipient of the Best Young Researcher in the Arab Student Forum Creative among 61 researchers from 16 countries at Alexandria University, Egypt, 2011. He has performed reviews for high prestigious journals, including IEEE TRANSACTIONS ON INDUSTRIAL INFORMATICS, IEEE TRANSACTIONS ON INDUSTRIAL ELECTRONICS, *Energy Conversion and Management*, *Applied Energy*, and *International Journal of Electrical Power and Energy Systems*.